치의과학박사 학위논문

The Role of NFIC and CPNE7 in Regulation of Cartilage Development and Dentin Regeneration

연골 발달과 상아질 재생에서 NFIC와 CPNE7의 역할

2022년 2월

서울대학교 대학원

치의과학과 세포 및 발생생물학 전공

노 송 이

The Role of NFIC and CPNE7 in Regulation of Cartilage Development and Dentin Regeneration

지도 교수 박 주 철

이 논문을 치의과학박사 학위논문으로 제출함
2021년 11월

서울대학교 대학원
치의과학과 세포 및 발생생물학 전공
노 송 이

노송이의 치의과학박사 학위논문을 인준함
2022년 01월

위 원 장 김 홍 희 (인)

부위원장 박 주 철 (인)

위 원 백 정 화 (인)

위 원 이 윤 실 (인)

위 원 김 정 희 (인)

The Role of NFIC and CPNE7 in Regulation of Cartilage Development and Dentin Regeneration

Directed by Prof. Joo-Cheol Park, D.D.S., Ph.D.

Submitting a Ph.D. Dissertation of Dentistry

November 2021

Graduate School of Dentistry
Seoul National University
Cell and Developmental Biology Major

Song Yi Roh

Confirming the Ph.D. Dissertation written by
Song Yi Roh

January 2022

Chair	Hong-Hee Kim
Vice Chair	Joo-Cheol Park
Examiner	Jeong-Hwa Baek
Examiner	Yun-Sil Lee
Examiner	Jeong-Hee Kim

Abstract

The Role of NFIC and CPNE7 in Regulation of Cartilage Development and Dentin Regeneration

Song Yi Roh
Cell and Developmental Biology Major
School of Dentistry
The Graduate School
Seoul National University
Directed by Prof. Joo-Cheol Park, D.D.S., Ph.D.

Growth plate chondrocytes are organized in parallel columns comprising resting, proliferative, pre-hypertrophic, and hypertrophic zones. A specialized cartilage matrix is deposited as chondrocytes mature and serves as a scaffold for blood vessels and osteoblasts to invade, leading to bone matrix accumulation (Arsenault et al. 1988; Hunziker et al. 1999; Noonan et al. 1998). Disruption in this multi-step differentiation process could lead to skeletal anomalies such as dwarfism (LuValle and Beier 2000).

Herein, the essential role of nuclear factor I C (NFIC) in

epiphyseal cartilage formation was demonstrated by examining the femoral growth-plate of *Nfic*-deficient mice. Chondrocyte proliferation was downregulated, and the number of apoptotic cell was increased in the growth plates of *Nfic*$^{-/-}$ mice. Further, the expression of the cell cycle inhibitor p21 was upregulated in the primary chondrocytes of *Nfic*$^{-/-}$ mice, whereas that of cyclin D1 was downregulated. These results suggest that NFIC may contribute to postnatal chondrocyte proliferation by inhibiting p21 expression and by increasing the stability of cyclin D1 protein.

During dentinogenesis, neural-crest derived ectomesenchymal stem cells differentiate into odontoblasts via sequential and reciprocal interaction with dental epithelium. Odontoblasts are polarized, highly specialized post-mitotic cells that are responsible for the dentin secretion. Besides their post-mitotic nature, the complex regulatory mechanism required for odontoblast differentiation has been considered as a big hurdle for tooth regeneration.

Copine 7 (CPNE7), a dental epithelium-derived factor, can re-activate dormant odontoblasts, and promote tubular tertiary dentin formation. In the present thesis, CPNE7 was suggested to promote tubular tertiary dentin formation by fine-tuning canonical Wnt signaling activity via modulation of β-catenin protein stability. Furthermore, the observed defects in primary ciliogenesis and altered expression of cell cycle regulators suggests a role for CPNE7

in cell cycle regulation during the terminal differentiation of odontoblasts.

Taken together, above studies suggest the essential roles of NFIC and CPNE7 during the epiphyseal chondrocyte proliferation and terminal odontoblast differentiation during dentin regeneration, respectively.

Keywords: Nfic, Cpne7, proliferation, differentiation, regeneration, odontoblasts, chondrocytes

Student Number: 2017-26174

Table of Contents

List of Figures

Abbreviations

ADP	Adenosine diphosphate
ALP	Alkaline phosphatase
aMEM	Alpha-modification of Eagle's medium
APC	Adenomatous polyposis coli
BMP-2	Bone morphogenic proteins
BMSC	Bone marrow stromal cell
BSA	Bovine serum albumin
β-TrCP	Beta-transducin repeats-containing proteins
CDK	Cyclin-dependent kinase
CIP	CDK-interacting protein
CK1	Casein kinase 1
ColX	Collagen type X
CPNE7	Copine-7
CT	Cycle threshold
DAB	3,3'-diaminobenzidine
DAPI	4',6-diamidino-2-phenylindole
DDW	Double distilled water
DSP	Dentin sialoprotein
DSPP	Dentin sialophosphoprotein
DMEM	Dulbecco's modified Eagle's medium
DMSO	Dimethyl Sulfoxide
DTCM	Dodecylthiocarbonyl-methyl
ECL	Enhanced chemiluminescence
ECM	Extracellular matrix

EMI	Epithelial-mesenchymal interaction
FBS	Fetal bovine serum
FBX4	F-box protein 4
FZ	Frizzled
GAPDH	Glyceraldehyde 3-phosphate dehydrogenase
GSK-3β	Glycogen Synthase kinase 3 beta
H&E	Hematoxylin and eosin
HECT	Homologous to the E6-AP carboxyl terminus
HIF-2α	Hypoxia-inducible factor 2 alpha
HCT	Human colon carcinoma cell line
IFT88	Intraflagella transport 88
IHC	Immunohistochemistry
INK	Inhibitors of CDK
KIF3α	Kinesin family member 3A
LEF1	Lymphoid enhancing factor 1
LRP	Low-density lipoprotein receptor-related protein
MDPC-23	Mouse dental papilla cell-23
mDPC	Mouse dental pulp cell
Micro-CT	Microcomputed tomography
MMP	Matrix metalloproteinase
MSC	Mesenchymal stem cell
NFIC	Nuclear factor I C
OD	Optical density
PARsylate	Poly (ADP)-ribosylate
PCNA	Proliferating cell nuclear antigen
PBS	Phosphate buffered saline

PFA	Paraformaldehyde
PMSF	Phenylmethylsulfonyl fluoride
POD	Peroxidase
rCPNE7	Recombinant copine 7
RING	Really interesting new gene
RIPA	Radioimmunoprecipitation assay
RT-PCR	Reverse transcription-polymerase chain reaction
SCF	Skp1, Cullins, F-box proteins
SKP2	S-phase kinase associated protein 2
SMAD	Small mothers against decapentaplegic
SMURF	Smad ubiquitin regulatory factor
TCF1	T-cell factor 1
TGF-β	Transforming growth factor beta
TNKS	Tankyrase
TUNEL	Terminal deoxynucleotidyl transferase-mediated biotin-dUTP nick-end labeling
VEGF	Vascular endothelial growth factor
vWA	Von Willebrand factor A
WAF	Wild-type p53-activated fragment

Chapter 1. Literature Review

I. Cell cycle control during endochondral bone formation

During development, bone formation could occur through two types of ossification: intramembranous and endochondral. Intramembranous bone formation is a characteristic way in which flat bones of the skull, mandible and clavicles are formed. During this process, osteoblasts are directly differentiated from mesenchymal stem cells (MSCs) and secret organic components of bone matrix.

On the other hand, endochondral bone formation involves the development of hyaline cartilage from aggregated MSCs, where the cartilage is subsequently replaced by bone (Horton 1990). Growth plate chondrocytes are organized in parallel columns comprising resting, proliferative, pre-hypertrophic, and hypertrophic zones. A specialized cartilage matrix is deposited as chondrocytes mature, and serves as a scaffold for blood vessels and osteoblasts to invade, leading to bone matrix accumulation (Arsenault et al. 1988; Hunziker et al. 1999; Noonan et al. 1998). Stringent regulation is, therefore, required to balance chondrocyte proliferation and differentiation during the longitudinal growth of long bone.

II. Nuclear factor I C in hard tissue formation

The nuclear factor I (NFI) family of transcription factors plays pivotal roles during the development of brain, muscles, lungs, and many other organs (Nagata et al. 1983). In vertebrates, the NFI family of transcription factors consists of four members, NFIA, NFIB, NFIC, and NFIX (Chaudhry et al. 1997; Gronostajski 2000). NFIA, NFIB, and NFIX deficient mice commonly exhibited some of the features such as high mortality rate and delayed glial and neuronal differentiation (Campbell et al. 2008; Shu et al. 2003; Steele-Perkins et al. 2005). *Nfic*-deficient mice, unlike those of other NFI family members, exhibited reduced bone density and defective tooth root formation whereas no life-threatening abnormalities were observed (Steele-Perkins et al. 2003). Previous in vivo and in vitro studies suggested that NFIC might function during the early stage of osteoblast differentiation, acting as a transcriptional switch during cell fate determination process to suppress adipogenic differentiation of bone marrow stromal cells (BMSCs) (Lee et al. 2014).

III. Tubular dentin formation

During tooth development, sequential and reciprocal epithelial-mesenchymal interaction allows odontoblasts to differentiate from ectomesenchymal cells of the dental papilla. As fully differentiated odontoblasts secret pre-dentin, odontoblast cell bodies are pulled towards the pulp chamber and mineralization occurs around the

elongated odontoblast process. Dentinal tubule, a minute canal structure that runs through nearly the entire length of dentin, is formed as a consequence. Dentin can be classified into three types: primary dentin is formed before tooth eruption, and secondary dentin is synthesized after eruption at a lower rate throughout lifetime (Bleicher 2014; Kuttler 1959). Tertiary dentin, on the other hand, is formed in response to external stimuli such as caries, microbial infection, and excessive wear. When damage is mild, the original odontoblasts survive and secret reactionary dentin that contain dentinal tubules (Thomas 1979). Upon severe trauma or deep cavity, original odontoblasts die, and new odontoblast-like cells are differentiated from pulp stem cells. Those newly formed cells secret atubular reparative dentin that exhibits bone like structure (Arana-Chavez and Massa 2004; Smith et al. 1995; Tziafas 1995).

IV. Wnt/β-catenin signaling pathway in dentinogenesis

Canonical Wnt signaling pathway mediates various biological processes such as cell proliferation, migration, and fate determination during development and homeostasis (Miller 2002). β-catenin is a protein with a dual function; it is a cell adhesion molecule (CAM) and a transducer within the canonical Wnt pathway (Behrens et al. 1996; Huber et al. 1996; Rimm et al. 1995). As global knockout of β-catenin resulted in embryonic lethality caused by gastrulation defects, researchers employed tissue specific knock out animal

models to reveal the importance of precise regulation of canonical Wnt activity for proper tooth and bone formation (Haegel et al. 1995). Many studies reported that activation of canonical Wnt signaling could promote odontoblast differentiation thus enhance tertiary dentin formation, while others demonstrated that persistent activation of canonical Wnt signaling led to disrupted odontoblast differentiation and dentinogenesis (Bae et al. 2013; Kim et al. 2011; Neves and Sharpe 2018; Scheller et al. 2008; Zhao et al. 2019).

V. Copine 7 in dentin regeneration

The copines (CPNE) are a family of highly conserved calcium-dependent phospholipid-binding proteins. Two N-terminal C2 domains (C2A and C2B) are responsible for the binding of phospholipid and intracellular proteins whereas a C terminal von Willebrand factor A (vWA)-domain can mediate protein-protein interactions (Creutz et al. 1998; Tomsig and Creutz 2002). Previous in vivo and in vitro studies revealed the essential functions of CPNE7 during odontoblast differentiation and tubular tertiary dentin formation (Oh et al. 2015; Park et al. 2019a; Park et al. 2019b; Seo et al. 2017). A recent report also suggested its ability in autophagic activity regulation to reactivate dormant, matured odontoblasts to secret dentin in indirect pulp capping model (Park et al. 2021).

VI. Rationale and outline of the thesis experiments

A key purpose of this thesis was to investigate 1) the essential role of NFIC in epiphyseal chondrocytes proliferation during postnatal cartilage development and 2) the underlying promotion mechanism of tubular tertiary dentin formation by CPNE7. Femoral growth plates of *Nfic* $^{-/-}$ mice were analyzed by micro-CT, IHC, and TUNEL assays, and primary chondrocytes from *Nfic* $^{-/-}$ mice were subjected for PCR, western blot, MTT assay, and DNA fragmentation assay to further elucidate the underlying mechanisms. Primary pulp cells were isolated from *Cpne7* $^{-/-}$ mice, and subjected for real time PCR, western blot, alizarin red S staining, and immunofluorescence analysis to reveal the modulation of β-catenin protein stability by CPNE7.

Chapter 2. NFIC is Required for Epiphyseal Chondrocyte Proliferation during Postnatal Cartilage Development

* This chapter has been largely reproduced from an article published by Song Yi Roh and Joo-Cheol Park

Molecules and Cells, 2020, Vol. 43, Issue 8, Pages 739-748

I. Introduction

Mesenchymal stem cells differentiate into osteoblasts, odontoblasts, adipocytes, and chondrocytes. They have diverse biological functions during pre- and postnatal development and growth; these functions are cell specific (Archer and Francis-West 2003). During the formation of long bone, primary ossification center appears within a cartilaginous scaffold at the future site of diaphysis as chondrocytes undergo hypertrophy. Secondary ossification center starts to form shortly after birth, compartmentalizing articular and growth-plate cartilage and establish epiphysis (Hall and Miyake 2000; Kronenberg 2003).

Chondrocytes in the epiphyseal growth plates differentiate to facilitate the longitudinal growth of long bones. Growth-plate chondrocytes are organized in parallel columns comprising resting, proliferative, prehypertrophic, and hypertrophic zones. When chondrocytes mature, a specialized cartilage matrix is deposited, which serves as a scaffold for blood vessels and osteoblasts to invade, leading to the accumulation of the bone matrix (Arsenault et al. 1988; Hunziker et al. 1999; Noonan et al. 1998). The formation of endochondral bone requires the stringent regulation of chondrocyte proliferation and differentiation. For example, skeletal anomalies, such as dwarfism, can occur when these two processes are not regulated (LuValle and Beier 2000). Regulators of the cell cycle play important roles in endochondral bone formation. Therefore, it is

essential to identify cell cycle genes and other factors, such as hormones and growth factors, that are involved in the regulation of cell cycle (Pines and Hurwitz 1991; Shum and Nuckolls 2002).

The nuclear factor I (NFI) family in vertebrates comprises NFIA, NFIB, NFIC, and NFIX, which bind as homo- or heterodimers to specific DNA sequences to regulate transcription (Gronostajski 2000; Kruse and Sippel 1994). NFIC functions as a key regulator during the postnatal development of hard tissues such as teeth and bones (Steele-Perkins et al. 2003). In *Nfic*$^{-/-}$ mice, *Nfic* deficiency severely inhibits the proliferation and differentiation of odontoblasts, leading to the formation of abnormal incisor dentin and short molar roots (Gronostajski 2000; Lee et al. 2009; Oh et al. 2012; Park et al. 2007). Postnatal bone formation and maintenance are affected by *Nfic* deficiency as well. The transcription of regulators of the cell cycle such as p21 and cyclin D1 is controlled by *Nfic* (Lee et al. 2014). Although considerable research has been devoted to identifying the function of NFIC in the formation and maintenance of hard tissue, less attention has been paid to NFIC's role in cartilage.

The aim of the present research therefore was to investigate the cause of defective growth and formation of cartilage in *Nfic*$^{-/-}$ mice, primarily focusing on the regulation of the transcription of cell cycle regulators by NFIC.

II. Materials and Methods

1. Mice

Experiments involving mice were performed according to the guidelines of the Dental Research Institute guidelines and Institutional Animal Care and Use Committee of Seoul National University (SNU-111013-2). *Nfic*$^{-/-}$ mice were generated by deletion of the second exon of *Nfic* (Gronostajski 2000). Homozygous *Nfic*$^{-/-}$ mice were obtained by crossing heterozygous *Nfic*$^{+/-}$ mice. The genotypes of the mice were determined as previously described (Steele-Perkins et al. 2003). As *Nfic*$^{-/-}$ mice have brittle teeth, a ground standard rodent chow was provided to all animals thrice a week beginning 3 days prior to weaning and continued for up to 6 weeks.

2. Microcomputed tomography (micro-CT) analysis, histology, and immunohistochemistry

The femurs of 6-week-old wild-type (WT) and *Nfic*$^{-/-}$ mice were removed, fixed in 4% paraformaldehyde at 4 °C overnight, and subjected to micro-CT using a SkyScan scanner and associated software (Skyscan 1172, Belgium). The isotopic resolution of the instrument is 10 μm. Decalcified femurs were embedded in paraffin and cut into sections 5-μm thick, stained using hematoxylin-eosin (H&E) and Alcian blue, and then analyzed using

immunohistochemistry (IHC) as previously described (Lee et al., 2009).

3. Cell culture and Transfection

ATDC5 cells (Riken Cell Bank, Japan) were cultured in DMEM/F12 supplemented with 100 IU/ml penicillin, 100 μg/ml streptomycin, and 5% fetal bovine serum (FBS; Life Technologies, USA). Primary chondrocytes were isolated from the growth plate of 6-week-old WT and *Nfic*$^{-/-}$ mice. Briefly, growth plates from distal femurs were dissected, washed in phosphate buffered saline (PBS), and digested with 1% Collagenase Type II (Gibco BRL, USA) and 1.6% Dispase II (Gibco BRL, USA) in Dulbecco's modified Eagle's medium: Nutrient mixture F-12 (DMEM/F12), for 1 h in an atmosphere containing 5% CO_2. The cells were cultured in DMEM/F12 supplemented with 100 IU/ml penicillin, 100 μg/ml streptomycin, and 5% FBS. Primary chondrocytes were incubated in the presence or absence of the proteasome inhibitor MG-132 at 5 μM (Sigma-Aldrich, USA) for 24 h. The *pCH-Nfic* expression plasmids were constructed as previously described (Lee et al., 2009), and the indicated expression plasmid (2 μg) was used to transiently transfect ATDC5 cells and primary chondrocytes in the presence of Lipofectamine Plus (Invitrogen, Carlsbad, USA) according to the manufacturer's instructions.

4. MTT assays

The proliferation rates of primary chondrocytes and ATDC5 cells were evaluated using MTT assays. Cells were seeded and cultured in 96-well plates (3×10^3 cells/well). After washing with PBS, 50 μl of MTT (5 mg/ml) was added to each well, which as then incubated for 4 h at 37 °C. After removing the MTT solution, the converted dye was dissolved in dimethyl sulfoxide (DMSO) and the absorbance at 540 nm was measured using a microplate reader (Multiskan EX, Finland). Triplicate samples from two independent experiments were analyzed.

5. Terminal deoxynucleotidyl transferase-mediated biotin-uDTP nick-end labeling (TUNEL) and DNA fragmentation assays

Apoptotic cells were identified using a TUNEL kit (Roche Biochemicals, Basel Switzerland), according to the manufacturer's instructions. Enzymatically labeled cells were incubated with the substrate 3,3'-diaminobenzidine tetrahydrochloride to yield a colored reaction product. For negative controls, the enzyme solution was omitted from the normal TUNEL procedures. For positive controls, cells were treated with DNase I (0.7 μg ml^{-1}; Gibco BRL, USA) for 10 min before TUNEL processing. The endogenous peroxidase within the tissue sections was inactivated by a 10-min incubation in 3% hydrogen peroxide (H_2O_2) before enzymatic labeling. Visualization of TUNEL staining was achieved by incubation with 3,3'-

diaminobenzidine (DAB) after enzymatic labeling, and the sections were counterstained with methyl green. DNA fragmentation assays were performed as previously described (Lee et al., 2012). Primary chondrocytes were collected 3 days after culturing commenced. Genomic DNA (gDNA) was isolated from primary chondrocytes using a gDNA isolation kit (Cosmo Genetech, Korea) according to the manufacturer's instructions. The gDNA (200 ng) was electrophoresed through 2% agarose gels, stained with ethidium bromide, and visualized using ultraviolet light.

6. Reverse transcription-polymerase chain reaction (RT-PCR) and real-time PCR analyses

Total RNA was extracted by using TRI reagent (MRC, Cincinnati, OH, USA), and 500ng of total RNA were reverse transcribed using Maxime^{TM} RT PreMix Kit (iNtRON Biotech, Seoul, Korea) at 45℃ for 1h and 95℃ 5 min. Real-time PCR was performed on an ABI PRISM 7500 sequence detection system (Applied Biosystems, Carlsbad, CA, USA) using the following pairs of primers: *Nfic*, forward 5'-GAC CTG TAC CTG GCC TAC TTT G-3' and reverse 5'- TGA AGA GGT CCT TGT CAT CCA G-3'; cyclin D1, forward 5'- CAC ACG GAC TAC AGG GGA GT-3' and reverse 5'- CAC AGG AGC TGG TGT TCC AT-3'; *Mmp9*, forward 5'- TGC CCA TTT CGA CGA CGA C-3' and reverse 5'- GTG CAG GCC GAA TAG GAG C-3'; *Mmp13*, forward 5'- TCC CTG CCC CTT CCC TAT GG-3' and reverse 5'- CCT CGG

AGC CTG TCA ACT GTG G-3'; and *Gapdh,* forward 5'- AGG TCG GTG TGA ACG GAT TTG -3' and reverse 5'- TGT AGA CCA TGT AGT TGA GGT CA-3', and ExcelTaq™ 2X Fast Q-PCR Master Mix (SMOBIO Technology Inc., Hsinchu, Taiwan) according to the manufacturer's instructions. All reactions were performed in triplicate, and the quantities of amplicons were normalized to those of *Gapdh*. Relative differences in PCR data were calculated using the comparative cycle threshold (CT) methods.

7. Western blot analysis

Western blot analyses were performed as previously described (Lee et al., 2009). Briefly, proteins (30 μg) were separated using 10% sodium dodecyl sulfate polyacrylamide gel electrophoresis, electrophoretically transferred onto a nitrocellulose membrane (Schleicher & Schuell BioScience, Germany), and incubated with the following antibodies: anti-NFIC (produced as previously described in Lee et al., 2011), anti-cyclin D1, anti-phospho-GSK3β (Ser9) (Cell Signaling Technology, USA), anti-PCNA, anti-p21, anti-SMURF1 and anti-SMURF2 (Santa Cruz Biotechnology, USA). Immunocomplexes were detected using an enhanced chemiluminescence system (GE Healthcare, Belgium).

8. Statistical analysis

All quantitative data are presented as the mean ± SD. The significance of differences was evaluated using the student *t* test ($*P < 0.05$).

III. Results

1. Decreased femoral growth-plate length in *Nfic*-deficient mice

To investigate the role of NFIC in chondrocyte proliferation and differentiation, we initially examined the effects of *Nfic* deficiency on developing femoral growth plates. 14-day-old *Nfic*$^{-/-}$ mice exhibited slightly reduced skeletal growth and decrease in growth plate thickness (Fig. 1). Correspondingly, 6-week-old *Nfic*$^{-/-}$ mice had slightly shorter femurs with narrower growth plates compared with those of WT mice (Fig. 2A and B). Histological analysis revealed decreased formation of growth cartilage and reduced thickness of the proliferating and hypertrophic zones (Fig. 2C). Histomorphometric analysis revealed a 49% decrease in growth-plate thickness, a 51% decrease in the length of the proliferating zone, a 44% decrease in the length of the hypertrophic zone, and a 60% decrease in cartilage thickness of *Nfic*$^{-/-}$ vs WT mice (Fig. 2C). There was no significant difference in prenatal cartilage formation (Fig. 3). These results suggest that *Nfic* deficiency caused abnormal postnatal proliferation and hypertrophy of chondrocytes, leading to reduced thickness of the epiphyseal cartilage and decreased growth.

A

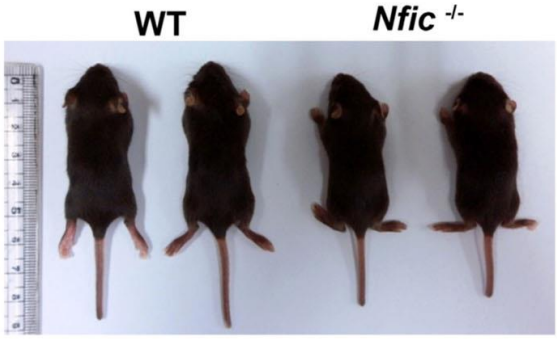
WT
Nfic -/-

B

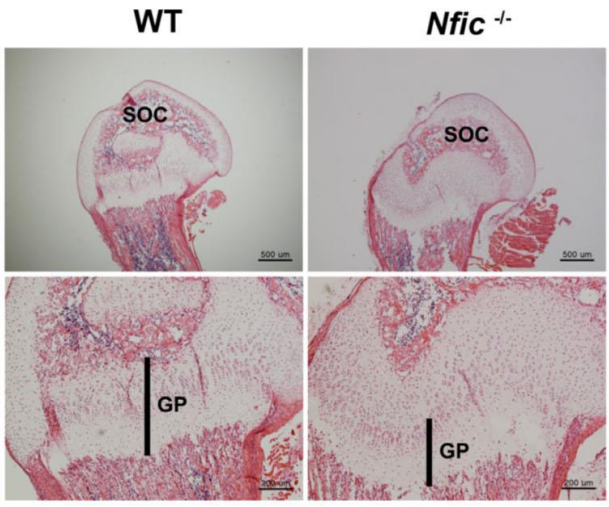
WT
Nfic -/-
SOC
SOC
500 um
500 um
GP
GP
200 um

C

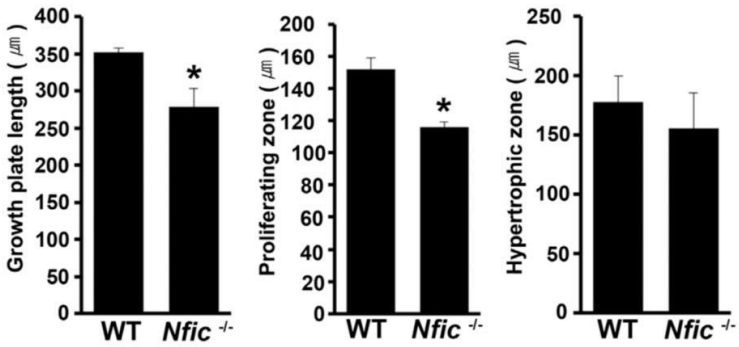
Growth plate length (μm)
400
350
300
250
200
150
100
50
0
*
WT
Nfic -/-
Proliferating zone (μm)
200
160
140
120
100
80
60
40
20
0
*
WT
Nfic -/-
Hypertrophic zone (μm)
250
200
150
100
50
0
WT
Nfic -/-

Figure 1. Reduced skeletal growth and decreased growth-plate thickness in 14-day-old *Nfic*$^{-/-}$ mice. (A) Appearances of 14-day-old mice. (B) Development of the growth plate was analyzed using H&E staining. Delayed formation of secondary ossification center is observed. Scale bars = 500 μm (top panels) and 200 μm (lower panels). (C) Histomorphometric analysis. Growth-plate length (left panel), lengths of the proliferating zone (middle panel), and the lengths of the hypertrophic zones (right panel); n = 3, *P < 0.05. Data are presented as the mean ± SD.

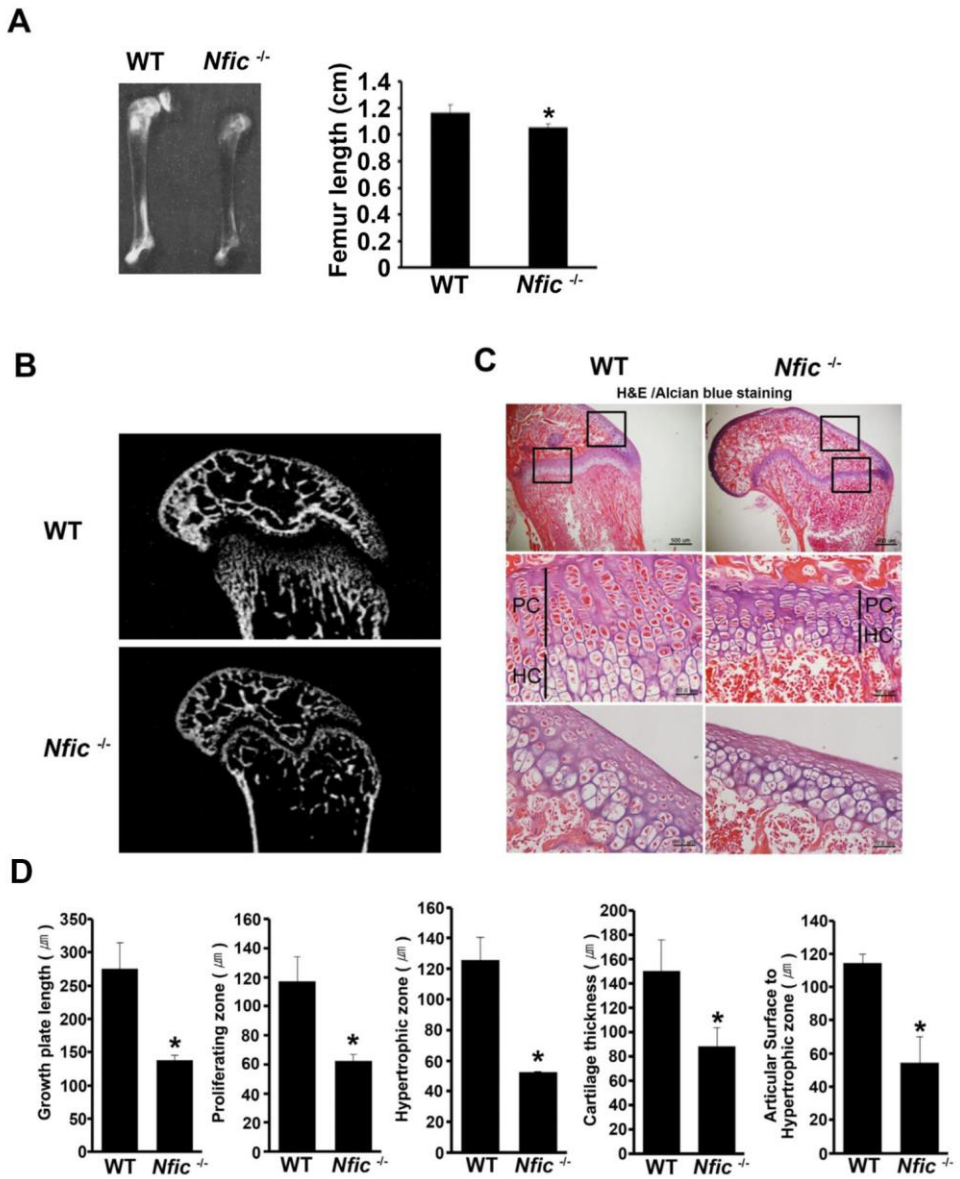

Figure 2. Decreased femur length and altered growth-plate morphology in 6-week-old *Nfic*$^{-/-}$ mice. (A) Representative X-ray image of the distal femur (left panel) and quantification of femur length (right panel). (B) Representative micro-CT image of the distal

femur. (C) Development of the growth plate in 6-week-old mice was analyzed using Alcian blue/H&E staining. Boxed areas in the upper panels show higher magnifications of the lower panels. PC, proliferating chondrocytes; HC, hypertrophic chondrocytes. Scale bars = 500 μm (top panels) and 50 μm (middle and bottom panels). (D) Histomorphometric analysis shows that the distance from the articular surface to the hypertrophic zone, growth-plate length, and the lengths of the proliferating zone and hypertrophic zones were significantly decreased in *Nfic*$^{-/-}$ mice compared with those of the WT (n = 3, *P < 0.05). Data represent the mean ± SD.

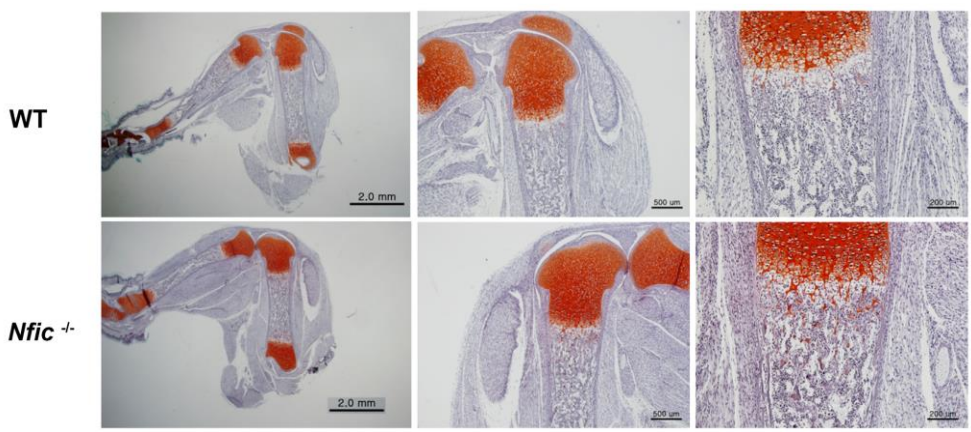

Figure 3. Effects of prenatal cartilage development in *Nfic*$^{-/-}$ mice. Safranin O staining of the femurs from WT and *Nfic*$^{-/-}$ mice on E18.5. Scale bars = 2.0 mm (left panels); 500 μm (middle panels); and 200 μm (right panels).

2. Downregulated chondrocyte proliferation in the femoral growth plate of *Nfic*-deficient mice

The changes in lengths of the proliferating and hypertrophic zones in growth-plate cartilage suggest that *Nfic* may be required for chondrocyte proliferation. To answer this question, PCNA levels were determined as an indicator of cell proliferation in the distal femurs of $Nfic^{-/-}$ mice. The number of PCNA-positive cells of the epiphyseal cartilage tissues of $Nfic^{-/-}$ mice decreased by ≥50% compared with those of WT mice (Fig. 4A). To further ascertain whether such defects in growth-plate cartilage were caused by *Nfic* deficiency, the proliferation of chondrocytes was analyzed. The proliferation of WT chondrocytes was indicated by the increased absorbance; however, $Nfic^{-/-}$ chondrocytes did not exhibit any significant increase in absorbance until day 5.

The levels of p21 and cyclin D1 were measured to further characterize the effects of *Nfic* deficiency on chondrocyte proliferation. The levels of p21 and cyclin D1 increased and decreased, respectively, suggesting that *Nfic* deficiency induced the growth arrest of chondrocytes (Fig. 4B). The effects of *Nfic* overexpression on the chondrocyte cell cycle was examined using the mouse chondroblast cell line ATDC5. Ectopic expression of *Nfic* increased chondrocyte proliferation, while decreasing p21 and increasing cyclin D1 levels, indicating that NFIC promoted the progression of the cell cycle (Fig. 4C). These data suggest that NFIC

may control the chondrocyte cell cycle by regulating the expression of p21.

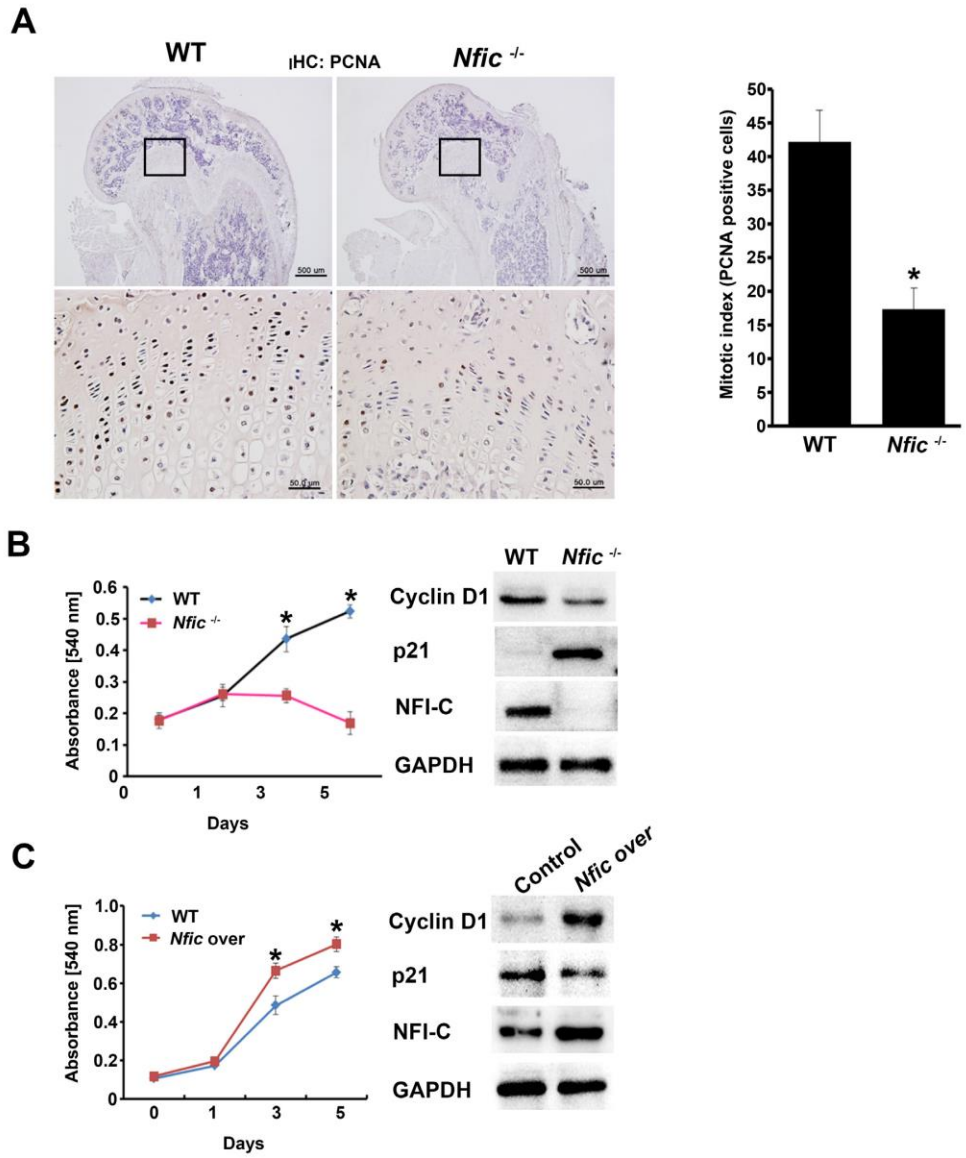

Figure 4. Decreased proliferation of chondrocytes in the growth plates of *Nfic*$^{-/-}$ mice. (A) Analysis of PCNA expression in the femurs of WT and *Nfic*$^{-/-}$ mice aged 6 weeks. Quantification of PCNA-positive cells in the growth plate of femurs of WT and *Nfic*$^{-/-}$ mice. Scale bars = 500 μm (top panels) and 50 μm (bottom panels). (B)

Primary chondrocytes isolated from the growth plate of the femurs of WT and *Nfic*$^{-/-}$ mice. Cell proliferation was measured using MTT assays on days 0, 1, 3, and 5 (upper panel). The expression of cyclin D1, p21, and NFIC were examined in ATDC5 cells by western blot analysis. (C) ATDC5 cells were transfected with an Nfic expression plasmid and cultured for 48 h. Cell proliferation was analyzed using an MTT assay. Western blot analysis of the expression of cyclin D1, p21, and NFIC ($n = 3$, $*P < 0.05$). Left panel, cell proliferation (MTT assay); Right panel, western blot analysis. Data represent the mean ± SD.

3. Increased chondrocyte apoptosis in the femoral growth plates of *Nfic*-deficient mice

We next determined if the decrease in overall length of the growth plate was caused by cell death. Apoptotic cells detected using the TUNEL POD assay were mainly present in the hypertrophic zone of *Nfic*$^{-/-}$ mice (Fig. 5A). DNA fragmentation assays revealed increased apoptosis of chondrocytes isolated from *Nfic*$^{-/-}$ vs WT mice (Fig. 5B). Activation of the effector caspase-3 is required for the activities of intrinsic and extrinsic apoptosis pathways. Western blot analysis detected upregulation of the levels of the precursor and active forms of caspase-3 in *Nfic*-deficient chondrocytes vs those of the WT (Fig. 5C). These results suggest that *Nfic* deficiency may induce caspase-dependent apoptosis of hypertrophic chondrocytes in growth plates.

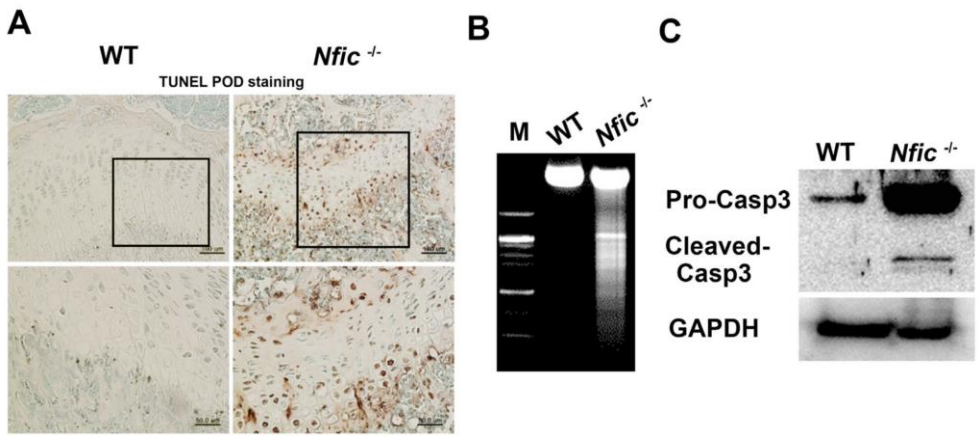

Figure 5. Increased apoptosis of growth-plate chondrocytes in *Nfic*$^{-/-}$ mice. (A) TUNEL POD analysis of apoptosis of growth-plate chondrocytes in femurs of 6-week-old WT and *Nfic*$^{-/-}$ mice. Boxed areas in the upper panels are shown at higher magnifications in the lower panels. Scale bars = 100 μm (top panels) and 50 μm (bottom panels). (B) DNA fragmentation analysis of cell death. Primary chondrocytes were isolated from the femur growth plates of WT and *Nfic*$^{-/-}$ mice. M, DNA size marker. (C) Western blot analysis of the expression pro-caspase-3 and cleaved caspase-3 in primary chondrocyte lysates of WT and *Nfic*$^{-/-}$ mice.

4. NFIC regulates the stability of cyclin D1 protein

To determine whether the overexpression of Nfic restored the levels of cyclin D1 in *Nfic*$^{-/-}$ mice to those of WT, primary chondrocytes were transfected with *Nfic* expression vectors. The levels of the mRNA encoding cyclin D1 did not significantly differ among WT, *Nfic*$^{-/-}$ chondrocytes, and transfected *Nfic*$^{-/-}$ chondrocytes (Fig. 6A). In contrast, cyclin D1 protein levels in transfected *Nfic*$^{-/-}$ chondrocytes were restored to those of WT (Fig. 6B). The discrepancy in the relative levels of mRNA and protein suggests that NFIC may regulate the protein stability of cyclin D1. To address this possibility, primary chondrocytes were incubated with the proteasome inhibitor MG-132 and subjected to western blot analysis. Cyclin D1 levels in primary chondrocytes from *Nfic*$^{-/-}$-deficient mice were upregulated upon MG-132 treatment, indicating that cyclin D1 levels in primary chondrocytes from the growth-plate cartilage of *Nfic*$^{-/-}$-mice were restored to those of WT by inhibiting proteasomal degradation (Fig. 6C). To gain further insight into the mechanism, we analyzed the expression of other proteins that may participate in the degradation of cyclin D1.

Glycogen synthase kinase-3 (GSK3) regulates cyclin D1 expression at the transcriptional and post-translational levels. Post-translational regulation is achieved via direct phosphorylation of cyclin D1, which is subsequently degraded (Diehl et al. 1998; Diehl et al. 1997; Reya and Clevers 2005). We found that the expression of

pGSK-3β, the inactive form of GSK-3β, was upregulated in primary chondrocytes of *Nfic*$^{-/-}$ mice vs those of WT. This result indicates that cyclin D1 protein expression was not likely regulated in a GSK-3β-dependent manner in *Nfic*$^{-/-}$ mice (Fig. 6C). Another candidate regulatory molecule called SMURF is a HECT-type E3 ubiquitin ligase that mediates NFIC degradation in odontoblasts. In *Nfic*$^{-/-}$ chondrocytes, SMURF1 (data not shown) and SMURF2 protein levels were upregulated compared with those of WT (Fig. 6D). This upregulation was inhibited by transfecting *Nfic*-expressing plasmids in *Nfic*$^{-/-}$ chondrocytes (Fig. 6E). When ATDC5 cells were transfected with Nfic expression vectors, *Smurf2* mRNA expression was downregulated (Fig. 6F). These findings indicate that NFIC may regulate cyclin D1 expression in chondrocytes via inhibition of proteasomal degradation, possibly through a SMURF2-mediated mechanism.

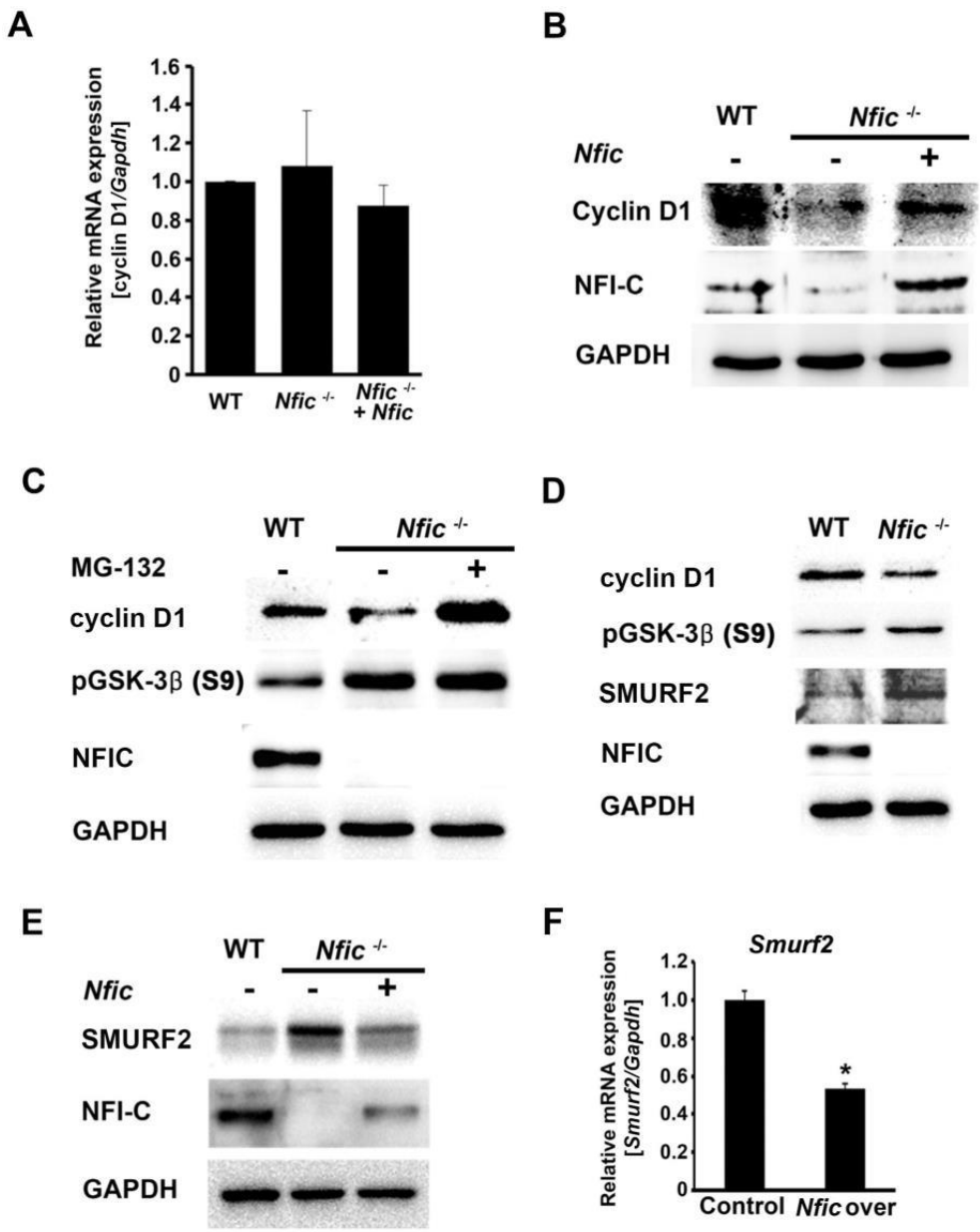

Figure 6. NFIC is required for the regulation of cyclin D1 protein stability in chondrocytes. (A) Real-time PCR analysis of the expression of cyclin D1 in primary WT and *Nfic*$^{-/-}$ chondrocytes. Primary chondrocytes were transfected with the *Nfic* expression

plasmid for 48 h. (B) Primary chondrocytes were transfected with the *Nfic* expression plasmid for 48 h. Western blot analysis of the expression of cyclin D1 and NFIC. (C) Primary chondrocytes were incubated in the presence or absence of the proteasome inhibitor MG-132 (5 μM) for 24 h. Western blot analysis of the expression of cyclin D1, pGSK-3β, and NFIC. (D) Western blot analysis of the expression of cyclin D1, pGSK-3β, and SMURF2. (E) Western blot analysis of SMURF2 expression. Primary chondrocytes were transfected with the *Nfic*-expressing plasmid for 48 h. (F) Real-time PCR analysis of the expression of *Smurf2*. ATDC5 cells were transfected with an *Nfic* expression plasmids and cultured for 48 h. n = 3, $*P < 0.05$. Data are presented as the mean ± SD.

5. Upregulated MMP9 and MMP13 levels in *Nfic*$^{-/-}$ mice chondroctyes

To investigate degradation and remodeling of the cartilage matrix during the endochondral bone formation, the expression of matrix metalloproteinase (MMP) family members was determined in *Nfic*$^{-/-}$ mice growth plate cartilage (Fig. 7A). The expression of *Mmp9* and *Mmp13* were upregulated at the transcriptional levels in primary chondroctyes and downregulated upon *Nfic* overexpression in ATDC5 cells (Fig. 7B and C). These results suggest that *Nfic* deficiency may lead to aberrant MMP expression and cause excess degradation of the cartilage ECM, resulting in defective cartilage formation in the growth plate.

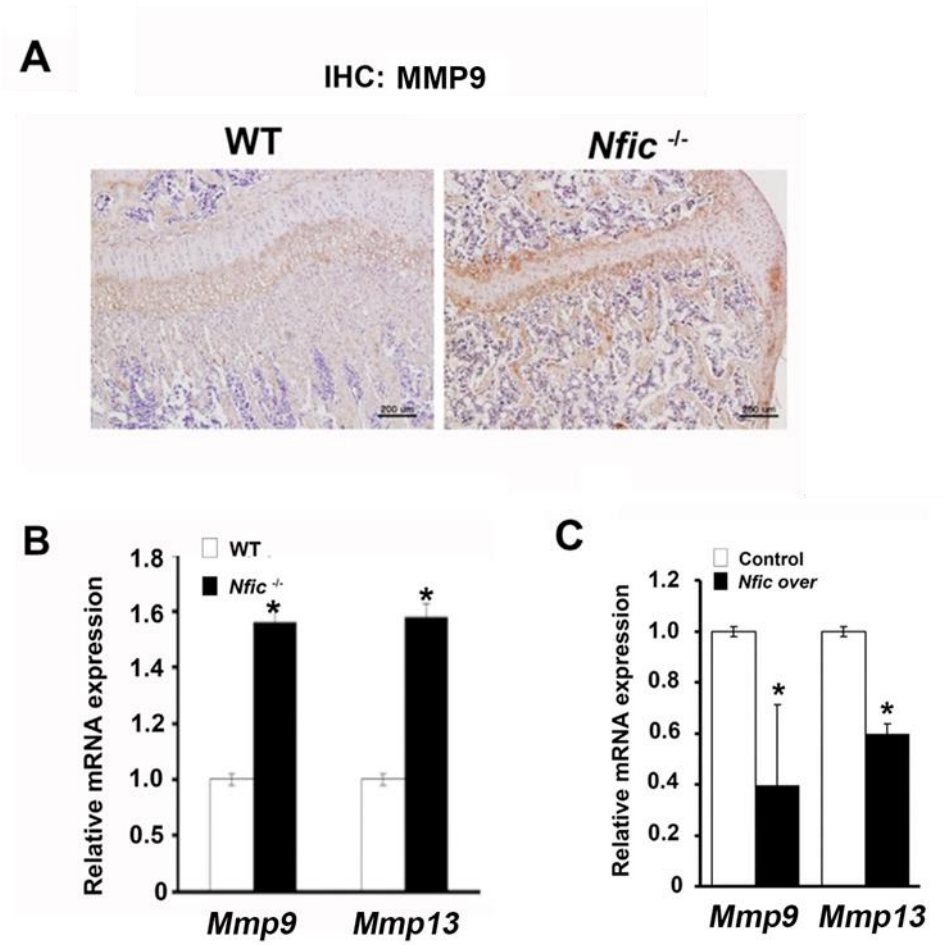

Figure 7. Expression of MMPs in *Nfic*$^{-/-}$ mice. (A) IHC analysis of MMP9 expression in the femurs of WT and *Nfic*$^{-/-}$ mice aged 6 weeks. Scale bars = 200 μm. (B) Real-time PCR analysis of the expression of mRNAs encoding *Mmp9* and *Mmp13* in primary chondrocytes. (C) Real-time PCR analysis of the expression of mRNA encoding *Mmp9* and *13* in ATDC5. ATDC5 cells were transfected with an *Nfic* expression plasmid and cultured for 48 h. n = 3, *P < 0.05. Data are presented as the mean ± SD.

IV. Discussion

This study demonstrated that postnatal deficiency of *Nfic* affects the development of the femoral growth plate. The reduced thickness of the proliferating and hypertrophic zones in *Nfic*$^{-/-}$ mice led us to analyze the expression of cell cycle regulators such as p21 and cyclin D1 to determine the function of NFIC in the formation and homeostasis of growth-plate cartilage. We show here that the levels of the mRNA encoding cyclin D1 were unaffected in primary chondrocytes isolated from *Nfic*$^{-/-}$ mice compared with those of WT mice. However, the protein levels of cyclin D1 in the former were significantly downregulated compared with those of WT. Moreover, ectopic expression of *Nfic* in *Nfic*$^{-/-}$ chondroyctes restored its levels to those of WT. These results suggest that the discrepancy in the levels of *Nfic* mRNA and protein was associated with regulation of the protein stability of cyclin D1 via NFIC.

The cell cycle is mainly regulated by cyclin-dependent kinases (CDK) in association with their partner proteins, the cyclins. During the G1–S phases of the cell cycle, decisions are made to proceed through the cell cycle and proliferate or to exit and arrest the cell cycle (Baldin et al. 1993; Ewen et al. 1993; Sherr 1993). Cyclin D1 forms a complex with cyclin-dependent kinase 4 (CDK4) or CDK6 to mediate the transition from G1 to S phase (Morgan 1997; Sherr 1995; Takahashi-Yanaga and Sasaguni 2008). Moreover, cyclin D1 is specifically expressed in proliferating chondrocytes and is

required for their proliferation. Further, cyclin D1-knockout mice exhibit a shortened growth-plate proliferative zone (Fantl et al. 1995; Yang et al. 2003; Zhang et al. 2009).

Cyclin D1 protein expression is regulated via a ubiquitin-dependent mechanism. Phosphorylated cyclin D1 is translocated from the nucleus to the cytoplasm where it undergoes degradation by the 26S proteasome. Evidence indicates that phosphorylation of cyclin D1 is mediated by GSK-3β, although other studies demonstrate that the degradation of cyclin D1 occurs in a GSK-3β-independent manner (Alao 2007; Diehl et al. 1998; Takahashi-Yanaga and Sasaguri 2008). For example, lithocholic acid hydroxyamide simultaneously up-regulates GSK-3β phosphorylation and down-regulates cyclin D1 protein expression in HCT116 cells (Magiera et al. 2017). These studies support our hypothesis that the stability of cyclin D1 is not regulated in a GSK-3β dependent manner in primary chondrocytes of *Nfic*$^{-/-}$ mice.

Regulation of the stability of cyclin D1 may be mediated instead via Smad ubiquitin regulatory factors (SMURFs). SMURFs are C2-WW-HECT-domain E3 ubiquitin ligases that regulate the components of the TGF-β and bone morphogenic protein (BMP) signal transduction pathways as well as others (Izzi and Attisano 2004; Waterfield 1991). SMURF1 negatively regulates the proliferation and differentiation of MSCs into osteoblasts. Upregulation of cyclin D1 expression occurs in *Smurf1*$^{-/-}$ MSCs (Zhao

et al. 2010), and *Smurf2* causes an osteoarthritis-like phenotype when overexpressed (Huang et al. 2016; Xing et al. 2010). In odontoblasts, SMURF1 mediates the ubiquitination and degradation of NFIC by forming an NFIC-SMAD2/3-SMURF complex (Lee et al. 2011a). Here we found that the upregulated expression of SMURF1 (data not shown) and SMURF2 in *Nfic*$^{-/-}$ chondrocytes suggests interactions between NFIC and SMURFs that regulate the proliferation of chondrocytes. Future research is therefore required to confirm whether SMURFs directly regulate the expression of cyclin D1. Similarly, SCF E3 ubiquitin ligases such as FBX4 and SKP2 are suggested to regulate the stability of cyclin D1; these ligases may interact with NFIC and these interactions need to be investigated (Ganiatsas et al. 2001; Lin et al. 2006; Russell et al. 1999).

In joint cartilage, TGF-β1 promotes matrix synthesis and prevents terminal differentiation of chondrocytes, and the expression of TGF-β1 is regulated in a temporospatial manner (Liu 2006; Ouellet et al. 2006). Interactions between TGF-β and NFIC may stringently regulate the expression of TGF-β during cartilage formation. Upregulated expression of p21 in hypertrophic chondrocytes suggests that p21 functions in the exit from the cell cycle and in the differentiation of chondrocytes (Stewart et al. 1997). p21$^{CIP1/Waf1}$ (p21) is one of the inhibitors of CDK (INK4) family that are capable of inactivating the cyclin-CDK complexes (Roussel 1999).

Interestingly, TGF-β and NFIC perform opposing functions in the regulation of p21 expression, and TGF-β induces the inhibition of cell proliferation by up-regulating the expression of p21 (Stewart et al. 1997). Moreover, NFIC inhibits the expression of p21 (Liu 2006; Ouellet et al. 2006). These findings suggest that the crosstalk between NFIC and TGF-β may regulate the proliferation and differentiation of chondrocytes via the regulation of p21 expression.

Degradation and remodeling of the cartilage matrix is essential during the formation of endochondral bone. Matrix metalloproteinase (MMP) family members cleave the major components of the cartilage ECM (Birkedal-Hansen et al. 1993; Werb 1997). Endochondral bone formation in mice deficient in MMP9 and MMP13 is severely impaired and is associated with decreased ECM remodeling and an expanded hypertrophic zone in the growth plate (Stickens et al. 2004; Vu et al. 1998). Here we show that in *Nfic*$^{-/-}$ mice the levels of MMP9 and MMP13 were upregulated at the transcriptional and translational levels in the growth plate. Further, a markedly shrunken hypertrophic zone morphology is consistent with previous observations. These findings suggest that *Nfic* deficiency may lead to aberrant MMP expression and cause excess degradation of the cartilage ECM, resulting in defective cartilage formation in the growth plate. Among the transcription factors that regulate MMP expressions, hypoxia-inducible factor 2 alpha (HIF-2α) shares an overlapping transcription factor binding site with NFIC near the

promoter region (Smythies et al. 2019). This raises an intriguing possibility that the interaction between HIF-2α and NFIC plays a role during cartilage development.

In summary, the results indicate that NFIC is essential for the postnatal proliferation of chondrocytes and cartilage formation in the growth plate cartilage. NFIC modulated the expression of cell cycle regulators such as p21 and cyclin D1 (Fig. 8). The stability of cyclin D1 protein was regulated via NFIC, and SMURFs may be involved. Further studies are warranted to identify the detailed mechanisms underlying the regulation of the protein stability of cyclin D1 by NFIC through SMURFs. Moreover, other factors and signaling pathways may interact with NFIC during cartilage formation, for example, SCF E3 ubiquitin ligases and the TGF-β signal transduction pathway as well as with MMP9, and MMP13. Further studies are required to confirm this hypothesis. Thus, it is reasonable to conclude that therapy targeting *Nfic* may contribute to the prevention and treatment of disorders caused by damage to cartilage and the associated growth defects.

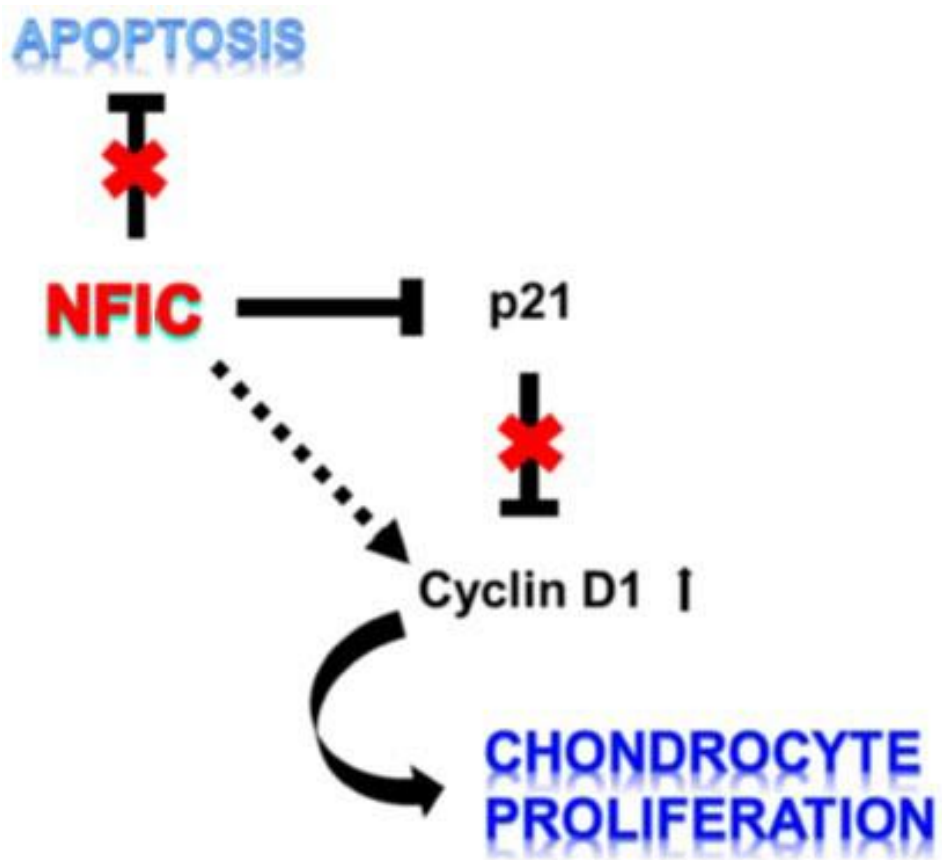

Figure 8. NFIC regulates chondrocyte proliferation by modulating the expression of p21 and cyclin D1. Schematic showing the function of NFIC during chondrocyte proliferation. NFIC regulates cyclin D1 expression by inhibiting p21 expression and modulating the protein stability of cyclin D1.

Chapter 3. CPNE7 Regulates Canonical Wnt Signaling Activity via Modulation of β-catenin Stability during Tertiary Dentin Formation

I. Introduction

Odontoblasts are neural crest-derived, postmitotic cells that are responsible for dentin formation. During tooth development, sequential and reciprocal epithelial-mesenchymal interactions allow odontoblasts to differentiate from ectomesenchymal stem cells. As fully differentiated odontoblasts secrete pre-dentin, odontoblast cell bodies are pulled toward the pulp chamber and mineralization occurs around the elongated odontoblast process. Dentinal tubules, minute canal structures that run through nearly the entire length of dentin, are subsequently formed (Thomas 1979). With odontoblast process within it, dentinal tubules allow odontoblasts to fulfil their sensory and protective function (Byers 1984; Farges et al. 2013; Hahn and Liewehr 2007; Maita et al. 1991; Pashley 1979; Thomas 1979). Dentin may be classified into three types. Primary dentin is synthesized before tooth eruption, whereas secondary dentin is formed after eruption at a lower rate throughout one's lifetime (Bleicher 2014; Kuttler 1959). Tertiary dentin is formed in response to external stimuli, such as caries, microbial infection, and excessive wear. Two types of tertiary dentinogenesis may occur depending on the intensity of the injury as it may alter odontoblast viability. During mild damage, existing odontoblasts survive and secrete physiological tubular dentin, which is known as reactionary dentin. In the event of severe trauma or deep cavity, the original odontoblasts die and pulp stem cells proliferate and differentiate into new odontoblast-like

cells to replace the original odontoblasts. Reparative dentin secreted by these newly differentiated odontoblast-like cells lacks dentinal tubules and exhibits a bone like structure, in which cells are entrapped in the dentin matrix (Arana-Chavez and Massa 2004; Smith et al. 1995; Tziafas 1995).

The Wnt/β-catenin signaling pathway mediates various biological processes such as cell proliferation, migration, and fate determination during development and homeostasis (Miller 2002). β-catenin is a dual function protein that plays a role in cadherin-based cell adhesion and the transduction of the canonical Wnt signaling pathway. Regulation of β-catenin expression is primarily achieved through a β-catenin destruction complex, which consists of glycogen synthase kinase 3α and 3β (GSK3α and 3β), adenomatous polyposis coli (APC), casein kinase 1 (CK1), and axin (Kimelman and Xu 2006). In the absence of Wnt ligands, β-catenin is phosphorylated by the β-catenin destruction complex and is subsequently ubiquitinated by β-TrCP, a substrate-binding subunit of the multiprotein Skp1-Cullin-F-box (SCF) RING type E3 ligase. Ubiquitinated β-catenin is subsequently targeted for proteasome-dependent degradation, thus β-catenin expression remains at a low level when Wnt signaling is off(Kimelman and Xu 2006; Stamos and Weis 2013). Upon binding of Wnt ligand to the receptor complex of transmembrane receptor proteins, frizzled (FZ) and low-density lipoprotein receptor-related protein (LRP) 5/6, β-catenin phosphorylation and subsequent

ubiquitination and degradation are suppressed, which results in β-catenin accumulation, nuclear translocation, and activation of Wnt target genes that regulate a wide range of physiological and developmental processes, such as cell proliferation and differentiation (Bhanot et al. 1996; Cadigan and Nusse 1997; Pinson et al. 2000). TNKS, a poly-(ADP)-ribose polymerases, are involved in various cellular processes including Wnt/β-catenin signaling pathway, telomere maintenance and vesicle trafficking (Cho-Park and Steller 2013; Cook et al. 2002; Hsiao and Smith 2008; Ozaki et al. 2012). TNKS activates canonical Wnt signaling by PARsylating axin, a concentration limiting component of β-catenin destruction complex (Huang et al. 2009; Kimelman and Xu 2006; Lee et al. 2003). While canonical Wnt/β-catenin signaling is indispensable for many biological processes, inappropriate activation of Wnt signaling can result in various diseases including cancer, aging, metabolic diseases, and neurodegenerative diseases (Clevers 2006; MacDonald et al. 2009). Previous studies have indicated that the stage-dependent activation and regulation of canonical Wnt signaling is required during the differentiation of many cell types including cortical progenitors, primordial germ cells, hair follicle stem cells, and osteoblasts (Bao et al. 2017; Huelsken et al. 2001; Le Rolle et al. 2021; Nakagawa et al. 2017).

The copines (Cpne) are a family of highly conserved calcium-dependent phospholipid-binding proteins. Consisted of two N-

terminal C2 domains (C2A and C2B) and a C-terminal von Willebrand factor A (vWA)-domain, these proteins are expected to be involved in membrane trafficking and protein-protein interactions (Creutz et al. 1998; Tomsig and Creutz 2002). Among family members, CPNE7 was shown to have major functions in odontoblast differentiation and physiological dentin formation. During odontogenesis, CPNE7 is secreted from inner dental epithelium and preameloblasts to differentiating odontoblasts, and promotes odontoblast differentiation and mineralization (Park et al. 2019b; Seo et al. 2017). Previous studies demonstrated that the application of recombinant CPNE7 (rCPNE7) and CPNE7-derived peptide to the exposed dentin not only promoted the formation of tubular tertiary dentin in the defect area, but also resulted in a significant decrease in microleakage (Choung et al. 2016; Lee et al. 2020; Park et al. 2019a). CPNE7-induced autophagic activity in old, inactive odontoblasts may play an essential role in this phenomenon (Park et al. 2021).

The aim of the present research was to investigate the detailed mechanism of physiological tertiary dentin formation by CPNE7, primarily focusing on the regulation of canonical Wnt signaling activity via CPNE7.

II. Materials and Methods

1. Mice

Experiments involving mice were performed according to the guidelines of the Dental Research Institute guidelines and Institutional Animal Care and Use Committee of Seoul National University (SNU-210205-1). *Cpne7* $^{+/-}$ mice were generated by deletion of the fifth, sixth, and seventh exons of *Cpne7* and the resulting heterozygous mice were crossed to obtain *Cpne7* $^{-/-}$ mice. The genotypes of the mice were determined by isolating genomic DNA from the tail tissue followed by RT-PCR analysis

2. Cell culture and transfection

Primary mouse dental pulp cells (mDPCs) were isolated from the mandibular incisors removed from 21-day-old (P21) wild type (WT) and *Cpne7* $^{-/-}$ mice. Isolated tissues were enzymatically digested in a mixture of 2 mg/ml type I collagenase and 2.5 mg/ml type II dispase (Gibco BRL, USA) at 37℃ for 50 min, and were dissociated by gentle pipetting. mDPCs were cultured in an alpha modification of Eagle's medium (αMEM; Life Technologies, USA) supplemented with 10% fetal bovine serum (FBS; Life Technologies, USA), 100 IU/ml penicillin, and 100 μg/ml streptomycin. MDPC-23 cells, provided by Dr. J.E. Nör (University of Michigan, Ann Arbor, MI), were cultured in Dulbecco's MEM (DMEM; Life Technologies, USA), supplemented

with 10% FBS, 100 IU/ml penicillin, and 100 μg/ml streptomycin. To induce odontogenic differentiation of mDPCs and MDPC-23 cells, 80–90% confluent cells were cultured in αMEM and DMEM, respectively, supplemented with 5% FBS, ascorbic acid (50 μg/ml), and β-glycerophosphate (10 mM) for up to 2 weeks. The expression plasmid for *Cpne7* was prepared as previously described (Lee et al. 2011b). Briefly, full-length mouse copine 7 (*Cpne7*) cDNA was generated by PCR, subcloned into the pCR® 2.1 TOPO vector (Invitrogen, USA), and subsequently ligated into the Hind III and EcoR V sites of the pcDNA3.1-HA vector (Invitrogen, USA). *Cpne7* siRNA-expression plasmid was prepared based on the chosen 19-nt of *Cpne7* (5'-AGGGTGTTCTGAAAGAAAT-3') using pSUPER-retro-neo-GFP siRNA-expression vector (OligoEngine, USA) according to the manufacturer's instructions. Each of those expression plasmid (2 μg) was transiently transfected into MDPC-23 cells using the Metafectene® Pro reagent (Biontex, Germany) according to the manufacturer's instructions.

3. Western blot analysis

Whole cell lysates were harvested using a radioimmunoprecipitation (RIPA) buffer containing 50 mM Tris-HCl, pH 7.4, 150 mM NaCl, 1 mM EDTA, 1% Nonidet P-14, 1 mM PMSF and supplemented with protease inhibitor cocktail tablets (Roche, Germany). Lysates were centrifuged at 13,000 x g for 30 min, and the supernatant was

collected. Protein concentration was determined using the DCTM protein assay system (Bio-Rad Laboratories, USA). Proteins (10 – 20 ug) were separated by 8 - 12% sodium dodecyl sulfate polyacrylamide gel electrophoresis, transferred onto polyvinylidene fluoride membranes (Merck, Darmstadt, Germany), and incubated with the following antibodies: anti-CPNE7, anti-DSP (produced as previously described in Lee et al., 2011), anti-β-catenin (N terminal), anti-phospho-β-catenin (Ser33/37/Thr41), anti-non-phospho (Active) β-catenin (Cell Signaling Technology, USA), anti-tankyrase 1/2, anti-ALP, anti-cyclin B1, anti-cyclin D1 (Santa Cruz Biotechnology, USA), anti-nestin, anti-GAPDH (Thermo Fisher Scientific, USA), anti-IFT88, anti-KIF3A (Proteintech, USA), anti-cyclin D1, anti-phospho-GSK3β (Ser9) (Cell Signaling Technology, USA), anti-PCNA, anti-p21, anti-SMURF1 and anti-SMURF2 (Santa Cruz Biotechnology, USA). The resulting immunocomplexes were detected using an enhanced chemiluminescence reagent (ECL; Santa Cruz Biotechnology) according to the manufacturer's instruction. Protein loading was assessed by GAPDH expression and quantified using ImageJ software (National Institute of Health, USA).

4. Real-time PCR

Total RNA was extracted by using TRI reagent (MRC, Cincinnati, OH, USA), and 500ng of total RNA were reverse transcribed using Maxime^{TM} RT PreMix Kit (iNtRON Biotech, Seoul, Korea) at 45℃ for

1h and 95℃ 5 min. Real-time PCR was performed on an ABI PRISM 7500 sequence detection system (Applied Biosystems, Carlsbad, CA, USA) using the following pairs of primers: *Cpne7*, forward 5'-AAT GCT GGC AAG TCC ACC ATC -3' and reverse 5'-TGA AGA GGT CCT TGT CAT CCA G-3'; *β-catenin*, forward 5'-ATG GAG CCG GAC AGA AAA GC-3' and reverse 5'-CTT GCC ACT CAG GGA AGG A-3'; *Tcf1*, forward 5'-CCT GCG GAT ATA GAC AGC ACT TC-3' and reverse 5'-TGT CCA GGT ACA CCA GAT CCC A-3'; *Lef1*, forward 5'-ACT GTC AGG CGA CAC TTC CAT G-3' and reverse 5'-GTG CTC CTG TTT GAC CTG AGG T-3'; cyclin D1, forward 5'-GCA GAA GGA GAT TGT GCC ATC C-3' and reverse 5'-AGG AAG CGG TCC AGG TAG TTC A-3'; *Dspp*, forward 5'-GTG AGG ACA AGG ACG AAT CTG A-3' and reverse 5'-CAC TAC TGT CAC TGC TGT CAC T-3'; nestin, forward 5'-CCC TGA AGT CGA GGA GCT G-3' and reverse 5'-CTG CTG CAC CTC TAA GCG A-3'; *Alp*, forward 5'-CCA ACT CTT TTG TGC CAG AGA-3' and reverse 5'-GGC TAC ATT GGT GTT GAG CTT TT-3'; *Ift88*, forward 5'- GCA GTG ACA GTG GCC AGA ACA ATA-3' and reverse 5'- CAG CCA GGG AGC AGA GAC AAG CAG-3'; *Kif3a*, forward 5'- GAA GCC CAA CAA GAG CAT CAG T-3' and reverse 5'- CCA GTG GAC GTA GTT TTC AAT CAT-3'; *Gapdh,* forward 5'- AGG TCG GTG TGA ACG GAT TTG -3' and reverse 5'- TGT AGA CCA TGT AGT TGA GGT CA-3', and ExcelTaq™ 2X Fast Q-PCR Master Mix (SMOBIO Technology Inc., Hsinchu, Taiwan) according to the manufacturer's

instructions. All reactions were performed in triplicate, and the quantities of amplicons were normalized to those of *Gapdh*. Relative differences in PCR data were calculated using the comparative cycle threshold (CT) methods.

5. Alizarin red S staining

Primary mDPCs were detached with 1xTE in PBS and sieved with cell strainers (SP Scienceware, USA). Then, 1 x 10^4 cells were seeded into 35 mm dishes and cultured in odontogenic media for the designated period of time. Cells were washed two times with 1x PBS and fixed with 4% PFA for 12 h. Fixed cells were briefly washed with 1x PBS and incubated with 40 mM alizarin red solution (pH 4.2) in the dark. After 30 min, the cells were washed five times in DDW and analyzed. The mineralized nodule was quantified by measuring OD405 values. Briefly, dishes were incubated for 30 min in 10 % acetic acid solution and homogenized by gentle pipetting. The mixture was heated to 85℃ for 10 min and cooled for 5 min on ice. The supernatant was collected by centrifugation at 20,000 x g for 15 min and neutralized with 10 % ammonium hydroxide.

6. Immunoflorescence

mDPCs were seeded and cultured on 12 mm cover glass (Deckglaser, Germany) for the designated period of time and washed thoroughly with PBS before fixing with 4% paraformaldehyde in PBS (T&I,

Korea). After permeabilizing with 0.5% Triton X-100 (Amresco, USA), the cells were washed with PBS, blocked with 2% BSA in 0.1% Tween 20 for 20 min, and then incubated with acetylated α-Tubulin (Proteintech, USA) diluted in 1% bovine serum albumin for 1 h. The cells were washed three times with 0.1% PBS-T and subsequently incubated with Cy3-conjugated rabbit IgG antibodies (1:200, Life Technologies) in the dark. After thorough washing with 0.5% Triton X-100, the cells were visualized by confocal laser scanning microscopy (Carl Zeiss, LSM 800, Germany).

7. Statistical analysis

All quantitative data are presented as the mean ± SD. The significance of differences was analyzed using a one-way analysis of variance or student's t test using Graphpad prism software (GraphPad Software Inc., USA) ($*p<0.05$).

III. Results

1. Sustained β-catenin expression during differentiation of *Cpne7*-deficient mDPCs.

To investigate the role of CPNE7 in odontoblast differentiation and tertiary dentin formation, the expression of odontogenic molecules during the differentiation of primary mDPCs was examined (data not shown). Of those molecules, β-catenin exhibited distinct protein expression patterns in *Cpne7* $^{-/-}$ mDPCs compared with those of the WT. In WT mDPCs, the total and active forms of β-catenin were downregulated throughout the differentiation period. In contrast, *Cpne7* $^{-/-}$ mDPCs exhibited relatively consistent expression levels, suggesting that *Cpne7* deficiency altered β-catenin protein expression during odontogenic differentiation (Fig. 9A). To confirm this, the odontoblast-like cell line, MDPC-23, were transfected with plasmids expressing *Cpne7* and *Cpne7*-siRNA, and subjected to western blot analysis and qPCR. *Cpne7* knock down caused a slight increase in total and active β-catenin protein expression. Overexpression of *Cpne7* resulted in a decrease in total and active β-catenin and an increase in inactive, phosphorylated β-catenin expression (Fig. 9B). In contrast, both *Cpne7* knock down and overexpression downregulated β-catenin mRNA. The expression of β-catenin target genes, such as cyclin D1, transcription factors T-cell factor 1 (*Tcf1*) and Lymphoid enhancing factor (*Lef1*), were

upregulated by *Cpne7* knock down and downregulated by *Cpne7* overexpression (Fig. 9C). These results suggest that the activity of Wnt/β-catenin signaling pathway was downregulated by *Cpne7*, possibly via modulation of β-catenin protein expression.

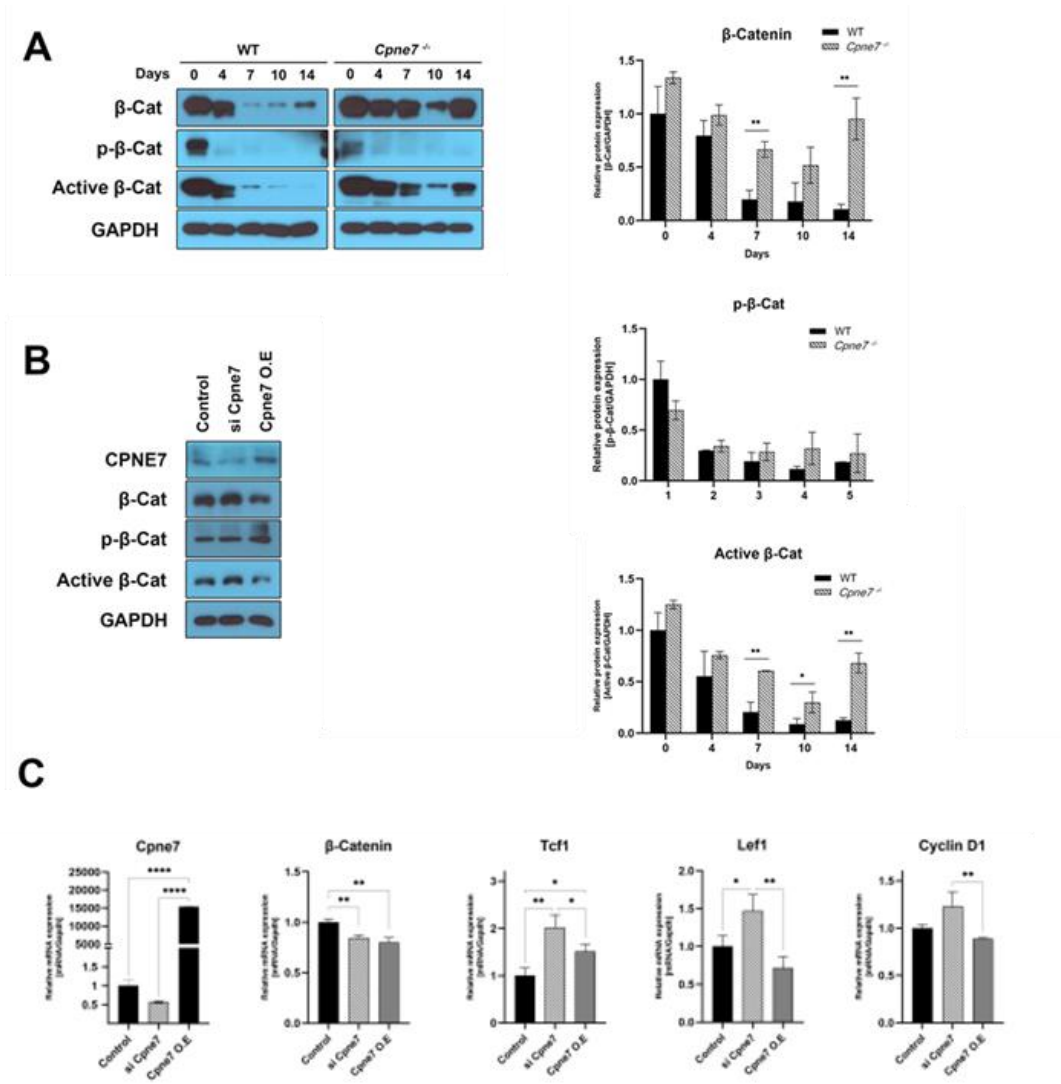

Figure 9. *Cpne7* deficiency caused upregulation in β-catenin protein expression and canonical Wnt signaling activity. (A) Western blot analysis of total, inactive, and active forms of β-catenin during differentiation periods of primary mDPCs from WT and *Cpne7* $^{-/-}$ mice. (B) MDPC-23 cells were transfected with *Cpne7*-siRNA and *Cpne7* expressing plasmids for 48 h and analyzed for the expression

of total, inactive, active forms of β-catenin and CPNE7. (C) MDPC-23 cells were transfected with *Cpne7* and *Cpne7*-siRNA expressing plasmids for 48 h and analyzed by real-time PCR. The mRNA expression of canonical Wnt target genes transcription factors T-cell factor 1 *(Tcf1)* and lymphoid enhancing factor 1 *(Lef1)* and cyclin D1 were upregulated by *Cpne7* deficiency. *Cpne7*, copine 7; mDPCs, mouse dental pulp cells; MDPC-23, mouse dental papilla cell-23. All values represent the mean ± standard deviation of three independently performed experiments (n = 3, *P < 0.05, **P < 0.001).

2. Defective mineralization in differentiating *Cpne7* $^{-/-}$ mDPCs

We next examined the effect of *Cpne7* deficiency in odontoblast differentiation and mineralization. The expression of the odontoblast differentiation marker, DSP, was upregulated as WT mDPCs differentiated, whereas its expression decreased after day 4 in *Cpne7* $^{-/-}$ mDPCs (Fig 10A). *Dspp* mRNA expression was also attenuated by *Cpne7* deficiency (Fig. 10B). Both the mRNA and protein expressions of nestin and ALP were also downregulated in differentiating *Cpne7* $^{-/-}$ mDPCs. The results from alizarin red S staining indicated reduced mineralization nodule formation in *Cpne7* $^{-/-}$ mDPCs (Fig. 10C and 11). These results suggest that the odontoblast differentiation and mineralization was affected by *Cpne7* deficiency.

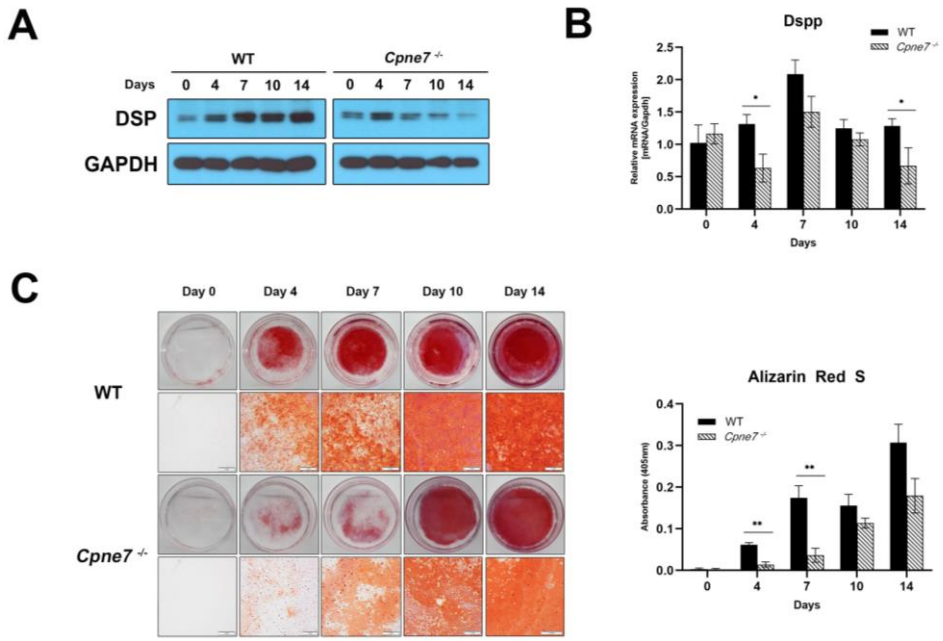

Figure 10. Decreased odontoblastic differentiation and mineralization in *Cpne7* $^{-/-}$ mDPCs. (A) Western blot analysis of an odontoblastic differentiation marker, dentin sialoprotein (DSP), during differentiation of *Cpne7* $^{-/-}$ mDPCs. Downregulation of DSP was noticeable, especially from day 7 of differentiation. (B) Real-time PCR analysis showing the decreased dentin sialophosphoprotein (*Dspp*) mRNA expression during differentiation of *Cpne7* $^{-/-}$ mDPCs. (C) Alizarin red S staining shows significantly decreased mineralization capacity in *Cpne7*-deficient mDPCs from the fourth day of differentiation. Stained mineralized nodules were quantified by ImageJ software. *Cpne7*, copine 7; mDPCs, mouse dental pulp cells. All values represent the mean ± standard deviation of three independently performed experiments (n = 3, *P < 0.05, **P < 0.001).

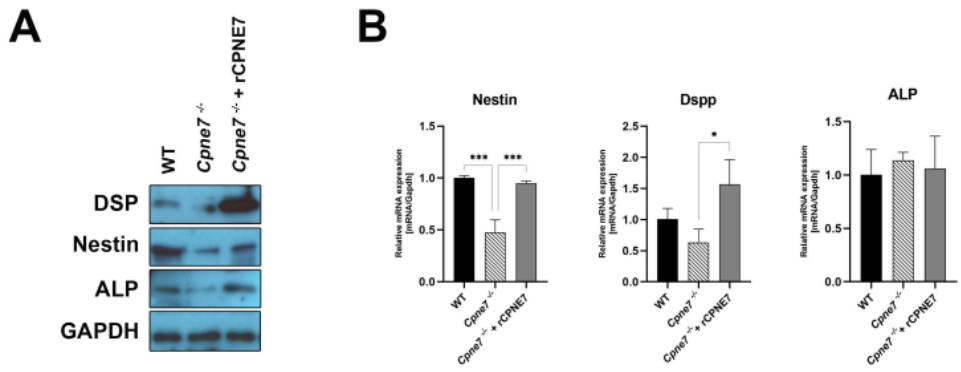

Figure 11. Decreased odontoblastic differentiation in *Cpne7* deficiency. (A) Western blot analysis of odontoblastic differentiation markers, dentin sialoprotein (DSP), nestin, and alkaline phosphatase (ALP) during differentiation of primary mDPCs. Primary mDPCs were cultured in odontogenic media with or without rCPNE7 treatment (100 ng/ml) for 4 days and analyzed by western blotting (B) and qPCR. The mRNA and protein expression of Dspp, nestin, and ALP was downregulated in Cpne7 deficiency, and upregulated upon rCPNE7 treatment in *Cpne7* $^{-/-}$ mDPCs. *Cpne7*, copine 7; mDPCs, mouse dental pulp cells; rCPNE7, recombinant copine 7; Dspp, dentin sialophosphoprotein. All values represent the mean ± standard deviation of three independently performed experiments (n = 3, *P < 0.05, **P < 0.001).

3. CPNE7 induces proteasomal degradation of β-catenin in MDPC-23 cells

To gain further insight into the mechanism of β-catenin regulation by CPNE7, we analyzed the expression of *β-catenin* during differentiation of primary mDPCs. No significant change was observed between WT and *Cpne7* $^{-/-}$ mDPCs (Fig. 12A). The regulation of β-catenin expression primarily occurs through the β-catenin destruction complex. β-catenin poly-phosphorylation leads to subsequent ubiquitylation and proteasomal degradation, maintaining Wnt/β-catenin signaling activity at a low level. β-catenin is rapidly degraded once phosphorylated by the destruction complex, thus MG-132, a proteasome inhibitor, was used to block the proteasomal degradation of phosphorylated β-catenin. When proteasome activity was blocked, the expression of the total and inactive forms of phospho-β-catenin were increased, whereas no significant change was observed in the *Cpne7* knock down group (Fig. 12B). These results suggest that CPNE7 participates in the β-catenin degradation process which involves phosphorylation, ubiquitination, and subsequent proteasome-dependent degradation.

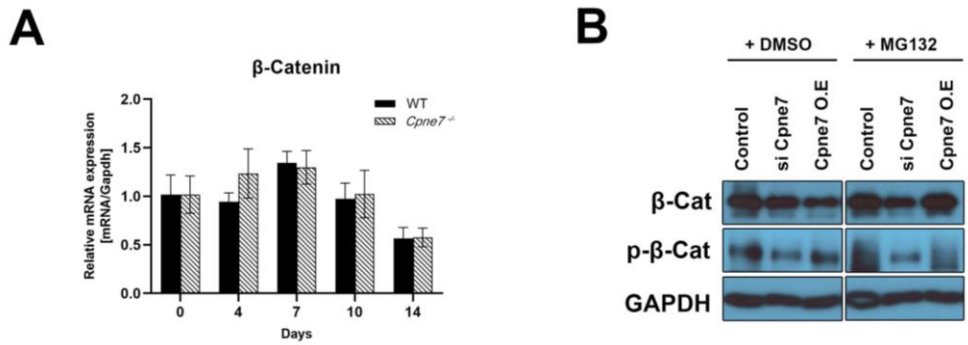

Figure 12. Proteasomal degradation of β-catenin was affected by *Cpne7* deficiency. (A) Real-time PCR analysis of *β-catenin* mRNA expression during the differentiation of mDPCs. No significant difference was observed between WT and *Cpne7* $^{-/-}$ mDPCs. All values represent the mean ± standard deviation of three independently performed experiments (n = 3, *P < 0.05). (B) MDPC-23 cells were transfected with *Cpne7* and *Cpne7*-siRNA expressing plasmids and incubated for 48 h. The cells were treated with dimethyl sulfoxide (DMSO) or 15 μM MG132 for 4 h. Western blot data indicates downregulated β-catenin phosphorylation and subsequent proteasome-dependent degradation in *Cpne7* deficiency. *Cpne7*, copine 7; mDPCs, mouse dental pulp cells; MDPC-23, mouse dental papilla cell-23.

4. Stage specific inhibition of tankyrase activity partially rescued mineralization in *Cpne7* $^{-/-}$ mDPCs.

To determine whether altered β-catenin destruction complex activity results in dysregulation of β-catenin protein stability in *Cpne7* $^{-/-}$ mDPCs, selected β-catenin destruction complex components were analyzed. Of these components, a noticeable difference in tankyrase 1/2 (TNKS1/2) expression was observed, which resembled that of total and active β-catenin in differentiating WT and *Cpne7* $^{-/-}$ mDPCs (Fig. 13A). We next promoted β-catenin destruction by inhibiting TNKS activity during the early and late stages of differentiation to determine if decreased mineralization could be rescued by inducing the degradation of excess β-catenin in *Cpne7* $^{-/-}$ mDPCs (Fig. 13B). When TNKS was inhibited through the third day of differentiation, mineralized nodule formation was decreased compared with that of the control group, whereas treatment with XAV-939 from day 4 to 14 slightly increased the mineralization capacity of *Cpne7* $^{-/-}$ mDPCs (Fig. 13C). These results suggest that CPNE7 modulates β-catenin protein stability by regulating β-catenin destruction complex activity, and TNKS may contribute to this process.

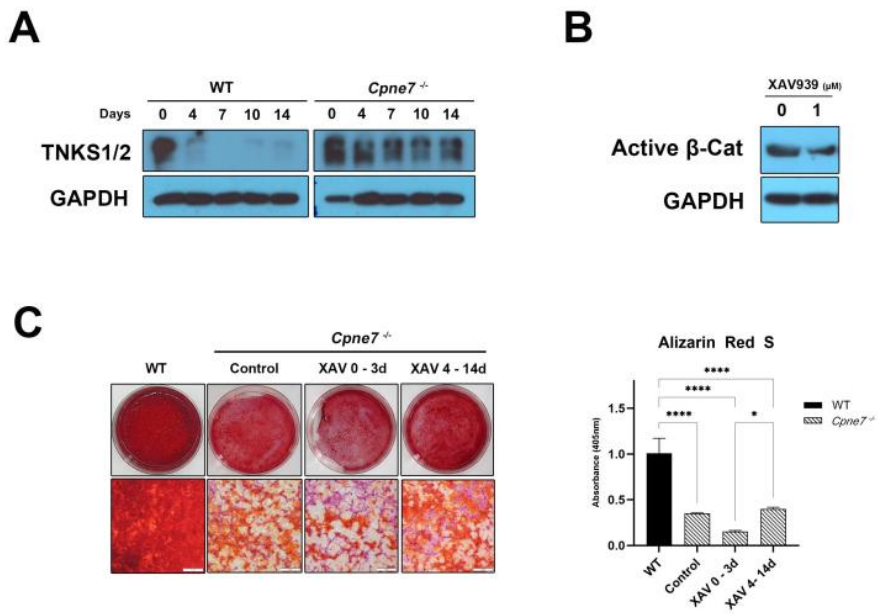

Figure 13. Inhibition of tankyrase during the late stage of odontoblastic differentiation partially rescues the mineralization capacity of *Cpne7* $^{-/-}$ mDPCs. (A) Western blot analysis shows the upregulation of tankyrase (TNKS) expression in differentiating *Cpne7* $^{-/-}$ mDPCs, compared with those of WT. (B) Active β-catenin protein expression was downregulated in MDPC-23 cells following treatment with 1 uM XAV939 for 48 h. (C) 1 uM XAV939 was added to odontogenic media for days 0-3 and 4-14 in *Cpne7* $^{-/-}$ mDPCs. Alizarin red S staining results indicate that inhibition of TNKS activity during the late stage of differentiation promoted mineralized nodule formation. Stained mineralized nodules were quantified by ImageJ software. *Cpne7*, copine 7; mDPCs, mouse dental pulp cells; MDPC-23, mouse dental papilla cell-23. All values represent the

mean ± standard deviation of three independently performed experiments (n = 3, *P < 0.05, **P < 0.001).

5. *Cpne7* deficiency altered the expression of cell cycle regulators and primary ciliogenesis.

To further investigate defective odontoblast differentiation in *Cpne7*-deficiency, the expression of cell cycle regulators was examined. Sustained cyclin D1 expression was observed throughout the differentiation periods in *Cpne7* $^{-/-}$ mDPCs (Fig. 14A). In MDPC-23 cells, *Cpne7* knock down resulted in an increase in cyclin D1 and B1 expression, whereas overexpression of *Cpne7* overexpression caused a decrease in cyclin D1 and B1 expression (Fig. 14B). Above result suggests the possible function of CPNE7 in cell cycle regulation. In postmitotic cells, primary cilia functions to prevent cells from re-entering the cell cycle, thus enabling cells to go through terminal differentiation and maintain their postmitotic status. Shortened primary cilia length along with the decrease in the number of ciliated cells were observed in *Cpne7* $^{-/-}$ mDPCs, which was rescued by treatment of rCPNE7 (Fig. 14C). Both the mRNA and protein expression of IFT88 and KIF3A, two of the major ciliary components, were downregulated in *Cpne7* $^{-/-}$ cells whereas treatment with rCPNE7 in *Cpne7* $^{-/-}$ cells partially restored the expression of these molecules (Fig. 14D and E).

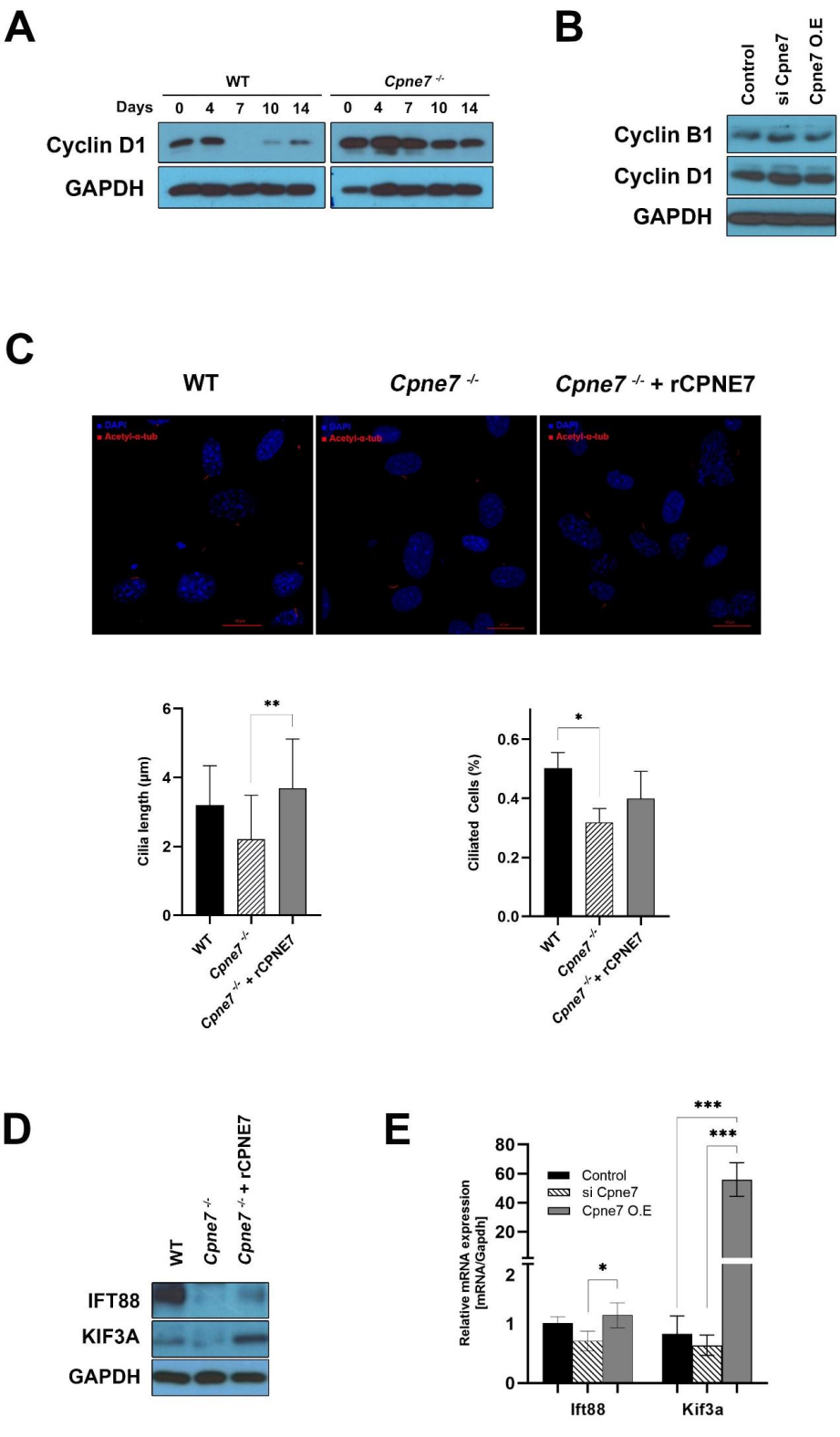
A
WT
Cpne7 -/-
Days
0 4 7 10 14
0 4 7 10 14
Cyclin D1
GAPDH
B
Control
si Cpne7
Cpne7 O.E
Cyclin B1
Cyclin D1
GAPDH
C
WT
Cpne7 -/-
Cpne7 -/- + rCPNE7
DAPI
Acetyl-α-tub
Cilia length (μm)
Ciliated Cells (%)
WT
Cpne7 -/-
Cpne7 -/- + rCPNE7
D
WT
Cpne7 -/-
Cpne7 -/- + rCPNE7
IFT88
KIF3A
GAPDH
E
Control
si Cpne7
Cpne7 O.E
Relative mRNA expression [mRNA/Gapdh]
Ift88
Kif3a

Figure 14. Sustained cyclin D1 expression and defective primary ciliogenesis in *Cpne7* $^{-/-}$ mDPCs. (A) Western blot analysis indicated upregulated cyclin D1 protein expression during the differentiation of primary *Cpne7* $^{-/-}$ mDPCs. (B) MDPC-23 cells were transiently tranfected with plasmids expressing *Cpne7* and *Cpne7*-siRNA, and harvested after 48 h. Western blot analysis suggests the regulation of cyclin B1 and cyclin D1 expression by *Cpne7*. (C) Primary mDPCs were cultured for 7 days in odontogenic media, with and without rCPNE7 treatment (100 ng/ml), and subjected to an immunofluorescence assay. Primary cilia were detected with acetylated α-tubulin immunostaining and were counterstained with DAPI (blue). Confocal images of primary cilia were captured and the length of primary cilia was measured using Olympus software. The percentage of ciliated cells was calculated using DAPI counterstaining. Scale bars = 20 μm. (D) Western blot analysis of IFT88 and KIF3A in primary mDPCs. (E) Real-time PCR analysis of the expression of *Kif3*α and *Ift88* in MDPC-23 cells. *Cpne7*, copine 7; mDPCs, mouse dental pulp cells; MDPC-23, mouse dental papilla cell-23; rCPNE7, recombinant copine 7; DAPI, 4',6-diamidino-2-phenylindole; IFT88, intraflagella transport 88; KIF3α, kinesin family member 3A. All values represent the mean ± standard deviation of three independently performed experiments (n=3, *P<0.05, **P<0.001).

IV. Discussion

Modulation of canonical Wnt/β-catenin signaling is of great interest to researchers in the field of dentin repair and regeneration. Many studies have demonstrated that canonical Wnt signaling regulates odontoblast differentiation and tooth morphogenesis (Chen et al. 2009; Kim et al. 2013; Zhang et al. 2013)(Han et al. 2014). Some studies, however, have shown that persistent expression of β-catenin inhibits differentiation and mineralization of dental pulp cells in vitro and causes premature differentiation of odontoblasts, which results in excessive globular dentin formation in vivo (Bae et al. 2013; Kim et al. 2011; Scheller et al. 2008).

During reparative dentinogenesis, odontoblast-like cells are differentiated from a pool of mesenchymal pulp stem cells to replace the severely damaged primary odontoblasts and secret reparative dentin, which lacks dentinal tubules. Upon damage to the dentin, rapid upregulation of Wnt/β-catenin signaling activity is observed in cells at the injury site (Han et al. 2014; Yoshioka et al. 2013). These Wnt active cells were shown to proliferate and differentiate into odontoblast-like cells in response to trauma. Inhibition of canonical Wnt signaling decreases proliferation activity, thus severely impairing tertiary dentin formation (Babb et al. 2017). A local upregulation of Wnt signaling at the injury site promotes tertiary dentinogenesis, yet the observed reparative dentin was atubular (Neves and Sharpe 2018; Zhao et al. 2019). Such discrepancies in

these findings indicate that canonical Wnt signaling activity needs to be intricately regulated, not only during tooth development, but also during tertiary dentinogenesis. To our knowledge, CPNE7 is the first bioactive molecule that was shown to promote odontoblastic differentiation of dental pulp cells and tubular physiological dentin formation in pulp capping dog models (Lee et al. 2020; Oh et al. 2012; Park et al. 2019a; Park et al. 2021; Seo et al. 2017). This study proposes that CPNE7 modulate β-catenin protein stability and fine-tune canonical Wnt signaling activity so that dental pulp stem cells could complete their terminal differentiation into fully functional odontoblasts and secret physiologic dentin.

Stringent regulation of cell cycle exit is required for the differentiation of postmitotic cells. Cyclin D1 forms a complex with CDK4 or CDK6 to mediate cell cycle progression (Shtutman et al. 1999). Thus, cyclin D1 downregulation is imperative for differentiation in many cell types including photoreceptor cells and osteoblasts (Bao et al. 2017; Wrobel et al. 2007). Since cyclin D1 is a direct transcriptional target of β-catenin/LEF1 complex, persistent β-catenin expression might upregulated cyclin D1 expression, inhibiting permanent cell cycle exit in differentiating *Cpne7* $^{-/-}$ cells. Primary ciliogenesis may participate in cell cycle regulation during odontoblastic differentiation. Primary cilium is a microtubule-based, non-motile extension of a centriole found on the surface of almost every eukaryotic cell type (Wheatley 1995). Assembly of primary

cilium is cell cycle-dependent and is usually induced during the G0 or G1 phase with a few exceptions (Plotnikova et al. 2009). In terminally differentiated cells, it functions to maintain their postmitotic status by preventing cells from re-entering the cell cycle (Walz 2017). Consistent with the work of Seo et al, immunofluorescence analysis demonstrated shortened cilia length along with a decrease in the number of ciliated cells in differentiating *Cpne7* $^{-/-}$ mDPCs. A recent study revealed a negative correlation between primary cilia and canonical Wnt signaling activity during dentinogenesis (Kawata et al. 2021; Wang et al. 2021). Taken together, we suggest that *Cpne7* deficiency causes a sustained activation of canonical Wnt signaling, which is possibly relevant to sustained cyclin D1 expression and defective primary ciliogenesis, thus leading to incomplete odontoblast differentiation (Fig. 15).

In summary, our results indicate that CPNE7 may promote the completion of odontoblast differentiation by fine-tuning canonical Wnt signaling. Further in vitro and in vivo studies are needed to identify the detailed mechanisms underlying the regulation of protein stability of β-catenin and TNKS by CPNE7, and its relevance to cell cycle regulation during tertiary dentin formation. Therefore, we believe that it is reasonable to conclude that targeting *Cpne7* may contribute to the regeneration of damaged dentin and associated defects.

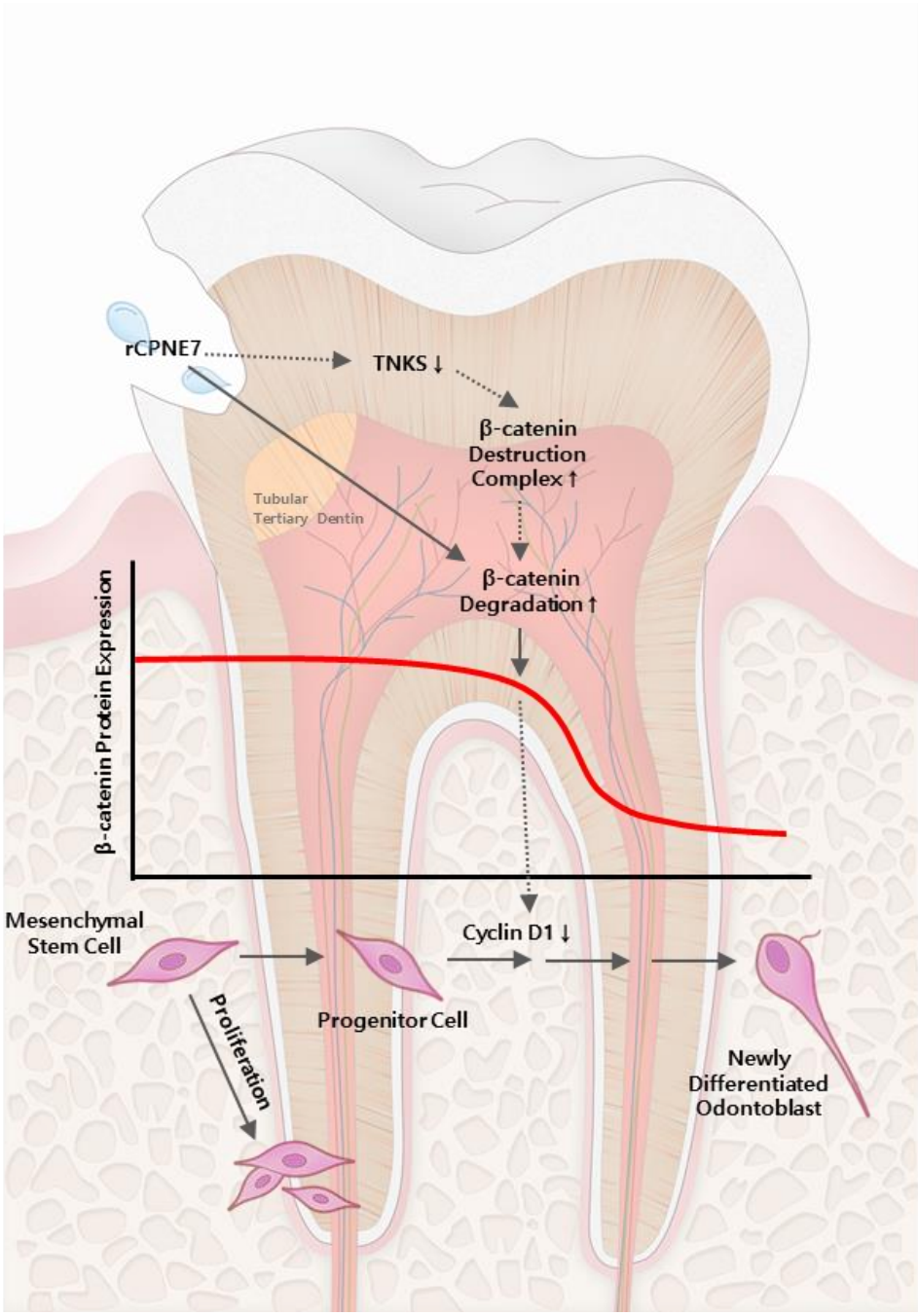

Figure 15. CPNE7 modulates β-catenin protein stability to regulate canonical Wnt signaling and promotes terminal differentiation of

odontoblasts. Schematic showing the effect of rCPNE7 treatment during tertiary dentin formation. CPNE7 modulates β-catenin protein stability, possibly via regulation of Tankyrases expression thus the activity of β-catenin destruction complex, and enables suppression of canonical Wnt at the appropriate time interval during odontogenic differentiation. Defective primary ciliogenesis and altered expression of cell cycle regulators in *Cpne7* deficiency also suggests the importance of cell cycle regulation for the terminal differentiation of odontoblasts.

Chapter 4. Concluding Remarks

The present thesis attempted to evaluate the role of NFIC and CPNE7 during epiphyseal cartilage formation and tertiary dentin formation, respectively.

Endochondral bone formation requires the stringent regulation of chondrocyte proliferation and differentiation. Although the importance of NFIC in hard tissue formation has been extensively investigated, knowledge regarding its biological roles and molecular mechanisms remains insufficient. Herein, the role of NFIC in epiphyseal cartilage formation was demonstrated by examining the femoral growth-plate of *Nfic*-deficient mice. Chondrocyte proliferation was downregulated and the number of apoptotic cell was increased in the growth plates of $Nfic^{-/-}$ mice. Further, the expression of the cell inhibitor p21 was upregulated in the primary chondrocytes of $Nfic^{-/-}$ mice, whereas that of cyclin D1 was downregulated. Therapy targeting Nfic, therefore, may contribute to the prevention and treatment of disorders caused by damage to cartilage and the associated growth defects.

Dentinogenesis requires precisely regulated temporo-spatial and reciprocal interactions between dental epithelium and mesenchyme. The complexity of this process makes it almost impracticable to recapitulate EMI, thus has been considered as a big hurdle for dentin regeneration. Canonical Wnt signaling is well known

for its essential function during odontoblast differentiation and tertiary dentin formation, yet simple activation or inhibition of canonical Wnt signaling is insufficient for physiological dentin regeneration. In this thesis, CPNE7 was suggested to fine-tune canonical Wnt signaling activity to promote tubular tertiary dentin formation. *Cpne7* deficiency results in persistent β-catenin protein expression and decreased differentiation and mineralization activity in dental pulp stem cells. Increased tankyrase expression and altered proteasome activity in *Cpne7*-deficient cells implicate the regulation of β-catenin protein stability by CPNE7. Furthermore, the observed defects in primary ciliogenesis and altered expression of cell cycle regulators suggests a role for CPNE7 in cell cycle regulation during the terminal differentiation of odontoblasts. Further in vitro and in vivo studies are warranted to identify the detailed mechanisms underlying the regulation of β-catenin and tankyrases protein stability by CPNE7, and its relevance to the cell cycle regulation during odontoblast differentiation.

Collectively, above studies provide the evidence for 1) the regulation of postnatal chondrocyte proliferation by NFIC and 2) the importance of canonical Wnt signaling modulation by CPNE7 during tertiary dentin formation.

References

Alao JP. 2007. The regulation of cyclin d1 degradation: Roles in cancer development and the potential for therapeutic invention. Mol Cancer. 6:24-40.

Arana-Chavez VE, Massa LF. 2004. Odontoblasts: The cells forming and maintaining dentine. Int J Biochem Cell Biol. 36(8):1367-1373.

Archer CW, Francis-West P. 2003. The chondrocyte. Int J Biochem Cell Biol. 35(4):401-404.

Arsenault AL, Ottensmeyer FP, Heath IB. 1988. An electron microscopic and spectroscopic study of murine epiphyseal cartilage: Analysis of fine structure and matrix vesicles preserved by slam freezing and freeze substitution. J Ultrastruct Mol Struct Res. 98(1):32-47.

Babb R, Chandrasekaran D, Carvalho Moreno Neves V, Sharpe PT. 2017. Axin2-expressing cells differentiate into reparative odontoblasts via autocrine wnt/beta-catenin signaling in response to tooth damage. Sci Rep. 7(1):3102.

Bae CH, Lee JY, Kim TH, Baek JA, Lee JC, Yang X, Taketo MM, Jiang R, Cho ES. 2013. Excessive wnt/beta-catenin signaling disturbs tooth-root formation. J Periodontal Res. 48(4):405-410.

Baldin V, Lukas J, Marcote MJ, Pagano M, Draetta G. 1993. Cyclin d1 is a nuclear-protein required for cell-cycle progression in g(1). Gene Dev. 7(5):812-821.

Bao Q, Chen S, Qin H, Feng J, Liu H, Liu D, Li A, Shen Y, Zhong X, Li J et al. 2017. Constitutive beta-catenin activation in osteoblasts impairs terminal osteoblast differentiation and bone quality. Exp Cell Res. 350(1):123-131.

Behrens J, von Kries JP, Kuhl M, Bruhn L, Wedlich D, Grosschedl R, Birchmeier W. 1996. Functional interaction of beta-catenin with the transcription factor lef-1. Nature. 382(6592):638-642.

Bhanot P, Brink M, Samos CH, Hsieh JC, Wang Y, Macke JP, Andrew D, Nathans J, Nusse R. 1996. A new member of the frizzled family from drosophila functions as a wingless receptor. Nature. 382(6588):225-230.

Birkedal-Hansen H, Moore WG, Bodden MK, Windsor LJ, Birkedal-Hansen B, DeCarlo A, Engler JA. 1993. Matrix metalloproteinases: A review. Crit Rev Oral Biol Med.

4(2):197-250.
Bleicher F. 2014. Odontoblast physiology. Exp Cell Res. 325(2):65-71.
Byers MR. 1984. Dental sensory receptors. Int Rev Neurobiol. 25:39-94.
Cadigan KM, Nusse R. 1997. Wnt signaling: A common theme in animal development. Genes Dev. 11(24):3286-3305.
Campbell CE, Piper M, Plachez C, Yeh YT, Baizer JS, Osinski JM, Litwack ED, Richards LJ, Gronostajski RM. 2008. The transcription factor nfix is essential for normal brain development. BMC Dev Biol. 8:52-80.
Chaudhry AZ, Lyons GE, Gronostajski RM. 1997. Expression patterns of the four nuclear factor i genes during mouse embryogenesis indicate a potential role in development. Dev Dyn. 208(3):313-325.
Chen J, Lan Y, Baek JA, Gao Y, Jiang R. 2009. Wnt/beta-catenin signaling plays an essential role in activation of odontogenic mesenchyme during early tooth development. Dev Biol. 334(1):174-185.
Cho-Park PF, Steller H. 2013. Proteasome regulation by adp-ribosylation. Cell. 153(3):614-627.
Choung HW, Lee DS, Lee JH, Shon WJ, Lee JH, Ku Y, Park JC. 2016. Tertiary dentin formation after indirect pulp capping using protein cpne7. J Dent Res. 95(8):906-912.
Clevers H. 2006. Wnt/beta-catenin signaling in development and disease. Cell. 127(3):469-480.
Cook BD, Dynek JN, Chang W, Shostak G, Smith S. 2002. Role for the related poly(adp-ribose) polymerases tankyrase 1 and 2 at human telomeres. Mol Cell Biol. 22(1):332-342.
Creutz CE, Tomsig JL, Snyder SL, Gautier MC, Skouri F, Beisson J, Cohen J. 1998. The copines, a novel class of c2 domain-containing, calcium-dependent, phospholipid-binding proteins conserved from paramecium to humans. J Biol Chem. 273(3):1393-1402.
Diehl JA, Cheng MG, Roussel MF, Sherr CJ. 1998. Glycogen synthase kinase 3 beta regulates cyclin d1 proteolysis and subcellular localization. Gene Dev. 12(22):3499-3511.
Diehl JA, Zindy F, Sherr CJ. 1997. Inhibition of cyclin d1 phosphorylation on threonine-286 prevents its rapid degradation via the ubiquintin-proteasome pathway. Gene Dev. 11(8):957-972.

Ewen ME, Sluss HK, Sherr CJ, Matsushime H, Kato JY, Livingston DM. 1993. Functional interactions of the retinoblastoma protein with mammalian d-type cyclins. Cell. 73(3):487-497.

Fantl V, Stamp G, Andrews A, Rosewell I, Dickson C. 1995. Mice lacking cyclin d1 are small and show defects in eye and mammary gland development. Genes Dev. 9(19):2364-2372.

Farges JC, Alliot-Licht B, Baudouin C, Msika P, Bleicher F, Carrouel F. 2013. Odontoblast control of dental pulp inflammation triggered by cariogenic bacteria. Front Physiol. 4:326-328.

Ganiatsas S, Dow R, Thompson A, Schulman B, Germain D. 2001. A splice variant of skp2 is retained in the cytoplasm and fails to direct cyclin d1 ubiquitination in the uterine cancer cell line sk-ut. Oncogene. 20(28):3641-3650.

Gronostajski RM. 2000. Roles of the nfi/ctf gene family in transcription and development. Gene. 249(1-2):31-45.

Haegel H, Larue L, Ohsugi M, Fedorov L, Herrenknecht K, Kemler R. 1995. Lack of beta-catenin affects mouse development at gastrulation. Development. 121(11):3529-3537.

Hahn CL, Liewehr FR. 2007. Innate immune responses of the dental pulp to caries. J Endod. 33(6):643-651.

Hall BK, Miyake T. 2000. All for one and one for all: Condensations and the initiation of skeletal development. Bioessays. 22(2):138-147.

Han N, Zheng Y, Li R, Li X, Zhou M, Niu Y, Zhang Q. 2014. Beta-catenin enhances odontoblastic differentiation of dental pulp cells through activation of runx2. PLoS One. 9(2):e88890. DOI: 10.1371/journal.pone.0088890.

Horton WC. 1990. Anterior zielke instrumentation for spinal deformity in adults. J Bone Joint Surg Am. 72(8):1268-1269.

Hsiao SJ, Smith S. 2008. Tankyrase function at telomeres, spindle poles, and beyond. Biochimie. 90(1):83-92.

Huang H, Veien ES, Zhang H, Ayers DC, Song J. 2016. Skeletal characterization of smurf2-deficient mice and in vitro analysis of smurf2-deficient chondrocytes. PLoS One. 11(1):e0148088. DOI: 10.1371/journal.pone.0148088

Huang SM, Mishina YM, Liu S, Cheung A, Stegmeier F, Michaud GA, Charlat O, Wiellette E, Zhang Y, Wiessner S et al. 2009. Tankyrase inhibition stabilizes axin and antagonizes wnt signalling. Nature. 461(7264):614-620.

Huber O, Korn R, McLaughlin J, Ohsugi M, Herrmann BG, Kemler R. 1996. Nuclear localization of beta-catenin by interaction with

transcription factor lef-1. Mech Dev. 59(1):3-10.
Huelsken J, Vogel R, Erdmann B, Cotsarelis G, Birchmeier W. 2001. Beta-catenin controls hair follicle morphogenesis and stem cell differentiation in the skin. Cell. 105(4):533-545.
Hunziker EB, Kapfinger E, Saager C. 1999. Hypertrophy of growth plate chondrocytes in vivo is accompanied by modulations in the activity state and surface area of their cytoplasmic organelles. Histochemistry and Cell Biology. 112(2):115-123.
Izzi L, Attisano L. 2004. Regulation of the tgf beta signalling pathway by ubiquitin-mediated degradation. Oncogene. 23(11):2071-2078.
Kawata K, Narita K, Washio A, Kitamura C, Nishihara T, Kubota S, Takeda S. 2021. Odontoblast differentiation is regulated by an interplay between primary cilia and the canonical wnt pathway. Bone. 150: e116001. DOI: 10.1016/j.bone.2021.116001
Kim TH, Bae CH, Lee JC, Ko SO, Yang X, Jiang R, Cho ES. 2013. Beta-catenin is required in odontoblasts for tooth root formation. J Dent Res. 92(3):215-221.
Kim TH, Lee JY, Baek JA, Lee JC, Yang X, Taketo MM, Jiang R, Cho ES. 2011. Constitutive stabilization of ss-catenin in the dental mesenchyme leads to excessive dentin and cementum formation. Biochem Biophys Res Commun. 412(4):549-555.
Kimelman D, Xu W. 2006. Beta-catenin destruction complex: Insights and questions from a structural perspective. Oncogene. 25(57):7482-7491.
Kronenberg HM. 2003. Developmental regulation of the growth plate. Nature. 423(6937):332-336.
Kruse U, Sippel AE. 1994. Transcription factor nuclear factor i proteins form stable homo- and heterodimers. FEBS Lett. 348(1):46-50.
Kuttler Y. 1959. Classification of dentine into primary, secondary, and tertiary. Oral Surg Oral Med Oral Pathol. 12(8):996-999.
Le Rolle M, Massa F, Siggers P, Turchi L, Loubat A, Koo BK, Clevers H, Greenfield A, Schedl A, Chaboissier MC et al. 2021. Arrest of wnt/beta-catenin signaling enables the transition from pluripotent to differentiated germ cells in mouse ovaries. Proc Natl Acad Sci U S A. 118(30):e2023376118. DOI: 10.1073/pnas.2023376118..
Lee DS, Choung HW, Kim HJ, Gronostajski RM, Yang YI, Ryoo HM, Lee ZH, Kim HH, Cho ES, Park JC. 2014. Nfi-c regulates osteoblast differentiation via control of osterix expression.

Stem Cells. 32(9):2467-2479.
Lee DS, Park JT, Kim HM, Ko JS, Son HH, Gronostajski RM, Cho MI, Choung PH, Park JC. 2009. Nuclear factor i-c is essential for odontogenic cell proliferation and odontoblast differentiation during tooth root development. J Biol Chem. 284(25):17293-17303.
Lee DS, Yoon WJ, Cho ES, Kim HJ, Gronostajski RM, Cho MI, Park JC. 2011a. Crosstalk between nuclear factor i-c and transforming growth factor-beta1 signaling regulates odontoblast differentiation and homeostasis. PLoS One. 6(12):e29160. DOI: 10.1371/journal.pone. 0029160
Lee E, Salic A, Kruger R, Heinrich R, Kirschner MW. 2003. The roles of apc and axin derived from experimental and theoretical analysis of the wnt pathway. PLoS Biol. 1(1):E10.
Lee JH, Lee DS, Choung HW, Shon WJ, Seo BM, Lee EH, Cho JY, Park JC. 2011b. Odontogenic differentiation of human dental pulp stem cells induced by preameloblast-derived factors. Biomaterials. 32(36):9696-9706.
Lee YS, Park YH, Lee DS, Seo YM, Lee JH, Park JH, Choung HW, Park SH, Shon WJ, Park JC. 2020. Tubular dentin regeneration using a cpne7-derived functional peptide. Materials (Basel). 13(20):4618. DOI: 10.3390/ma13204618
Lin DI, Barbash O, Kumar KG, Weber JD, Harper JW, Klein-Szanto AJ, Rustgi A, Fuchs SY, Diehl JA. 2006. Phosphorylation-dependent ubiquitination of cyclin d1 by the scf(fbx4-alphab crystallin) complex. Mol Cell. 24(3):355-366.
Liu F. 2006. Smad3 phosphorylation by cyclin-dependent kinases. Cytokine Growth Factor Rev. 17(1-2):9-17.
LuValle P, Beier F. 2000. Cell cycle control in growth plate chondrocytes. Front Biosci. 5:D493-503.
MacDonald BT, Tamai K, He X. 2009. Wnt/beta-catenin signaling: Components, mechanisms, and diseases. Dev Cell. 17(1):9-26.
Magiera K, Tomala M, Kubica K, De Cesare V, Trost M, Zieba BJ, Kachamakova-Trojanowska N, Les M, Dubin G, Holak TA et al. 2017. Lithocholic acid hydroxyamide destabilizes cyclin d1 and induces g0/g1 arrest by inhibiting deubiquitinase usp2a. Cell Chem Biol. 24(4):458-470 e418.
Maita E, Simpson MD, Tao L, Pashley DH. 1991. Fluid and protein flux across the pulpodentine complex of the dog in vivo. Arch Oral Biol. 36(2):103-110.
Miller JR. 2002. The wnts. Genome Biol. 3(1):REVIEWS3001. DOI:

10.1186/ gb-2001-3-1-reviews3001
Morgan DO. 1997. Cyclin-dependent kinases: Engines, clocks, and microprocessors. Annu Rev Cell Dev Bi. 13:261-291.
Nagata K, Guggenheimer RA, Hurwitz J. 1983. Adenovirus DNA replication in vitro: Synthesis of full-length DNA with purified proteins. Proc Natl Acad Sci U S A. 80(14):4266-4270.
Nakagawa N, Li J, Yabuno-Nakagawa K, Eom TY, Cowles M, Mapp T, Taylor R, Anton ES. 2017. Apc sets the wnt tone necessary for cerebral cortical progenitor development. Genes Dev. 31(16):1679-1692.
Neves VCM, Sharpe PT. 2018. Regulation of reactionary dentine formation. J Dent Res. 97(4):416-422.
Noonan KJ, Hunziker EB, Nessler J, Buckwalter JA. 1998. Changes in cell, matrix compartment, and fibrillar collagen volumes between growth-plate zones. J Orthop Res. 16(4):500-508.
Oh HJ, Choung HW, Lee HK, Park SJ, Lee JH, Lee DS, Seo BM, Park JC. 2015. Cpne7, a preameloblast-derived factor, regulates odontoblastic differentiation of mesenchymal stem cells. Biomaterials. 37:208-217.
Oh HJ, Lee HK, Park SJ, Cho YS, Bae HS, Cho MI, Park JC. 2012. Zinc balance is critical for nfi-c mediated regulation of odontoblast differentiation. J Cell Biochem. 113(3):877-887.
Ouellet S, Vigneault F, Lessard M, Leclerc S, Drouin R, Guerin SL. 2006. Transcriptional regulation of the cyclin-dependent kinase inhibitor 1a (p21) gene by nfi in proliferating human cells. Nucleic Acids Res. 34(22):6472-6487.
Ozaki Y, Matsui H, Asou H, Nagamachi A, Aki D, Honda H, Yasunaga S, Takihara Y, Yamamoto T, Izumi S et al. 2012. Poly-adp ribosylation of miki by tankyrase-1 promotes centrosome maturation. Mol Cell. 47(5):694-706.
Park JC, Herr Y, Kim HJ, Gronostajski RM, Cho MI. 2007. Nfic gene disruption inhibits differentiation of odontoblasts responsible for root formation and results in formation of short and abnormal roots in mice. J Periodontol. 78(9):1795-1802.
Park SH, Lee YS, Lee DS, Park JC, Kim R, Shon WJ. 2019a. Cpne7 induces biological dentin sealing in a dentin hypersensitivity model. J Dent Res. 98(11):1239-1244.
Park YH, Lee YS, Park JS, Kim SH, Bae HS, Park JC. 2019b. Expression of cpne7 during mouse dentinogenesis. J Mol Histol. 50(3):179-188.
Park YH, Son C, Seo YM, Lee YS, Har A, Park JC. 2021. Cpne7-

induced autophagy restores the physiological function of mature odontoblasts. Front Cell Dev Biol. 9:e655498. DOI: 10.3389/fcell.2021.655498
Pashley DH. 1979. The influence of dentin permeability and pulpal blood flow on pulpal solute concentrations. J Endod. 5(12):355-361.
Pines M, Hurwitz S. 1991. The role of the growth plate in longitudinal bone growth. Poult Sci. 70(8):1806-1814.
Pinson KI, Brennan J, Monkley S, Avery BJ, Skarnes WC. 2000. An ldl-receptor-related protein mediates wnt signalling in mice. Nature. 407(6803):535-538.
Plotnikova OV, Pugacheva EN, Golemis EA. 2009. Primary cilia and the cell cycle. Methods Cell Biol. 94:137-160.
Reya T, Clevers H. 2005. Wnt signalling in stem cells and cancer. Nature. 434(7035):843-850.
Rimm DL, Koslov ER, Kebriaei P, Cianci CD, Morrow JS. 1995. Alpha 1(e)-catenin is an actin-binding and -bundling protein mediating the attachment of f-actin to the membrane adhesion complex. Proc Natl Acad Sci U S A. 92(19):8813-8817.
Roussel MF. 1999. The ink4 family of cell cycle inhibitors in cancer. Oncogene. 18(38):5311-5317.
Russell A, Thompson MA, Hendley J, Trute L, Armes J, Germain D. 1999. Cyclin d1 and d3 associate with the scf complex and are coordinately elevated in breast cancer. Oncogene. 18(11):1983-1991.
Scheller EL, Chang J, Wang CY. 2008. Wnt/beta-catenin inhibits dental pulp stem cell differentiation. J Dent Res. 87(2):126-130.
Seo YM, Park SJ, Lee HK, Park JC. 2017. Copine-7 binds to the cell surface receptor, nucleolin, and regulates ciliogenesis and dspp expression during odontoblast differentiation. Sci Rep. 7(1): e11283. DOI: 10. 1038/s41598-017-11641-y
Sherr CJ. 1993. Mammalian g1 cyclins. Cell. 73(6):1059-1065.
Sherr CJ. 1995. D-type cyclins. Trends Biochem Sci. 20(5):187-190.
Shu T, Butz KG, Plachez C, Gronostajski RM, Richards LJ. 2003. Abnormal development of forebrain midline glia and commissural projections in nfia knock-out mice. J Neurosci. 23(1):203-212.
Shum L, Nuckolls G. 2002. The life cycle of chondrocytes in the developing skeleton. Arthritis Res. 4(2):94-106.
Smith AJ, Cassidy N, Perry H, Begue-Kirn C, Ruch JV, Lesot H. 1995.

Reactionary dentinogenesis. Int J Dev Biol. 39(1):273-280.
Smythies JA, Sun M, Masson N, Salama R, Simpson PD, Murray E, Neumann V, Cockman ME, Choudhry H, Ratcliffe PJ et al. 2019. Inherent DNA-binding specificities of the hif-1alpha and hif-2alpha transcription factors in chromatin. EMBO Rep. 20(1): e46401. DOI: 10.15252/embr.201846401
Stamos JL, Weis WI. 2013. The beta-catenin destruction complex. Cold Spring Harb Perspect Biol. 5(1):a007898. DOI: 10.1101/cshperspect.a007898
Steele-Perkins G, Butz KG, Lyons GE, Zeichner-David M, Kim HJ, Cho MI, Gronostajski RM. 2003. Essential role for nfi-c/ctf transcription-replication factor in tooth root development. Mol Cell Biol. 23(3):1075-1084.
Steele-Perkins G, Plachez C, Butz KG, Yang G, Bachurski CJ, Kinsman SL, Litwack ED, Richards LJ, Gronostajski RM. 2005. The transcription factor gene nfib is essential for both lung maturation and brain development. Mol Cell Biol. 25(2):685-698.
Stewart MC, Farnum CE, MacLeod JN. 1997. Expression of p21cip1/waf1 in chondrocytes. Calcif Tissue Int. 61(3):199-204.
Stickens D, Behonick DJ, Ortega N, Heyer B, Hartenstein B, Yu Y, Fosang AJ, Schorpp-Kistner M, Angel P, Werb Z. 2004. Altered endochondral bone development in matrix metalloproteinase 13-deficient mice. Development. 131(23):5883-5895.
Takahashi-Yanaga F, Sasaguni T. 2008. Gsk-3 beta regulates cyclin d1 expression: A new target for chemotherapy. Cellular Signalling. 20(4):581-589.
Takahashi-Yanaga F, Sasaguri T. 2008. Gsk-3beta regulates cyclin d1 expression: A new target for chemotherapy. Cell Signal. 20(4):581-589.
Thomas HF. 1979. The extent of the odontoblast process in human dentin. J Dent Res. 58(Spec Issue D):2207-2218.
Tomsig JL, Creutz CE. 2002. Copines: A ubiquitous family of ca(2+)-dependent phospholipid-binding proteins. Cell Mol Life Sci. 59(9):1467-1477.
Tziafas D. 1995. Basic mechanisms of cytodifferentiation and dentinogenesis during dental pulp repair. Int J Dev Biol. 39(1):281-290.
Vu TH, Shipley JM, Bergers G, Berger JE, Helms JA, Hanahan D,

Shapiro SD, Senior RM, Werb Z. 1998. Mmp-9/gelatinase b is a key regulator of growth plate angiogenesis and apoptosis of hypertrophic chondrocytes. Cell. 93(3):411-422.
Walz G. 2017. Role of primary cilia in non-dividing and post-mitotic cells. Cell Tissue Res. 369(1):11-25.
Wang W, Jack BM, Wang HH, Kavanaugh MA, Maser RL, Tran PV. 2021. Intraflagellar transport proteins as regulators of primary cilia length. Front Cell Dev Biol. 9:e661350. DOI: 10.3389/fcell.2021.661350
Waterfield MD. 1991. Peptide growth-factors and their receptors, vol 1-2 - sporn,mb, roberts,ab. Nature. 350(6319):566-566.
Werb Z. 1997. Ecm and cell surface proteolysis: Regulating cellular ecology. Cell. 91(4):439-442.
Wheatley DN. 1995. Primary cilia in normal and pathological tissues. Pathobiology. 63(4):222-238.
Wrobel CN, Mutch CA, Swaminathan S, Taketo MM, Chenn A. 2007. Persistent expression of stabilized beta-catenin delays maturation of radial glial cells into intermediate progenitors. Dev Biol. 309(2):285-297.
Xing L, Zhang M, Chen D. 2010. Smurf control in bone cells. J Cell Biochem. 110(3):554-563.
Yang Y, Topol L, Lee H, Wu J. 2003. Wnt5a and wnt5b exhibit distinct activities in coordinating chondrocyte proliferation and differentiation. Development. 130(5):1003-1015.
Yoshioka S, Takahashi Y, Abe M, Michikami I, Imazato S, Wakisaka S, Hayashi M, Ebisu S. 2013. Activation of the wnt/beta-catenin pathway and tissue inhibitor of metalloprotease 1 during tertiary dentinogenesis. J Biochem. 153(1):43-50.
Zhang M, Xie R, Hou W, Wang BL, Shen R, Wang XM, Wang Q, Zhu TH, Jonason JH, Chen D. 2009. Pthrp prevents chondrocyte premature hypertrophy by inducing cyclin-d1-dependent runx2 and runx3 phosphorylation, ubiquitylation and proteasomal degradation. Journal of Cell Science. 122(9):1382-1389.
Zhang R, Yang G, Wu X, Xie J, Yang X, Li T. 2013. Disruption of wnt/beta-catenin signaling in odontoblasts and cementoblasts arrests tooth root development in postnatal mouse teeth. Int J Biol Sci. 9(3):228-236.
Zhao L, Huang J, Guo R, Wang Y, Chen D, Xing L. 2010. Smurf1 inhibits mesenchymal stem cell proliferation and differentiation into osteoblasts through junb degradation. J

Bone Miner Res. 25(6):1246-1256.
Zhao Y, Yuan X, Bellido T, Helms JA. 2019. A correlation between wnt/beta-catenin signaling and the rate of dentin secretion. J Endod. 45(11):1357-1364 e1351.

국문초록

연골 발달과 상아질 재생에서 NFIC와 CPNE7의 역할

중간엽 줄기세포의 응집 (condensation)과 분화를 통해 만들어진 골단의 성장판 연골세포 (epiphyseal growth plate chondrocyte)는 장골 (long bone)의 지속적인 길이 성장을 담당한다. 본 연구에서는 nuclear factor I C (*Nfic*)의 결핍이 넓적다리 뼈의 성장판 형성에 미치는 영향에 대해 밝혔다. *Nfic*가 결핍된 쥐의 성장판에서 연골세포의 증식이 감소하고 사멸세포 (apoptotic cell)의 수가 증가했으며, 세포 주기 억제 인자인 p21 발현의 증가와 cyclin D1 발현의 감소가 관찰되었다. 본 연구를 통해 NFIC가 p21을 억제하고 cyclin D1 단백질의 안정성을 증가시킴으로써 생후 연골세포의 증식에 관여할 가능성이 있음을 밝혔다.

치아 형성 과정동안 상아모세포(odontoblast)는 신경능선세포 기원의 외배엽성 미분화중간엽세포 (ectomesenchymal stem cell)로부터 분화한다. 유사핵분열중지(postmitotic) 세포인 상아모세포로의 완전한 분화는 치성 상피와 간엽 간의 순차적인 상피간엽상호작용(epithelial mesenchymal interaction, EMI)의 정밀한 조절을 필요로 하는데, 아직까지는 그 조절 기전의 재현을 통한 생리적 상아질 재생이 불가능하기 때문에 관련 연구가 계속해서 이뤄지고 있다. 치성 상피에서 유래한 인자인 copine 7 (CPNE7)은 생체 내에서 삼차 상아질 형성을 유도하고, 생체 외 배양 실험에서 상아모세포의 분화와 석회화를 유도한다고 보고되어 있다.

본 연구에서는 CPNE7이 β-catenin 단백질의 안정성 조절을 통해 Wnt 신호전달 체계의 활성을 조절함으로써 상아세관을 가진 삼차상아질의 형성에 기여할 가능성이 있음을 밝혔다. CPNE7에 의한 Wnt 신호전달 체계 활성 조절은 세포주기의 조절과도 연관이 있는데, 분화 과정 동안 상아모세포의 유사핵분열중지 상태를 유지시킴으로써 최종 분화(terminal differentiation)를 유도할 가능성에 대해서도 보고했다.

총괄적으로, 위의 연구들은 NFIC와 CPNE7이 성장판 연골모세포의 증식 및 분화 과정과, 중간엽 줄기세포로부터 상아모세포가 분화하는 과정에서 각각 중요한 역할을 할 가능성을 시사한다.

주요어: Nfic, Cpne7, 증식, 분화, 재생, 상아모세포, 연골세포

학 번: 2017-26174